History and Status of the CDISC Aerodynamic Design Method

Richard L. Campbell[1], Michelle N. Banchy[2], and Brett R. Hiller[3]
NASA Langley Research Center, Hampton, Virginia, 23681

This paper will review the development and application of the CDISC aerodynamic design method that began in the early 1980s and continues in active use today. The method uses an iterative, knowledge-based approach that has been coupled with numerous flow solvers utilizing a variety of grid types and levels of flow physics. It has been applied to configurations varying in complexity from 2D airfoils to full 3D aircraft at flow conditions ranging from low-speed, high-lift to supersonic cruise. The knowledge-based approach provides a very rapid design process, with designs typically completed in approximately 1-2x the time required for an initial converged analysis of the baseline. The evolution of the method as it tracked the expansive growth of grid and flow solver technology, along with some major applications over five decades, are given, followed by a description of the philosophy and process used in design. Finally, an example of its use in a preliminary design environment is given.

Nomenclature

Acronyms

AATT = Advanced Air Transport Technology
AAVP = Advanced Air Vehicles Program
ALMA = Aft Laminar Multielement Airfoil
ARMD = Aeronautics Research Mission Directorate
AST = Advanced Subsonic Transport program
BLI = Boundary-Layer Ingestion
BLSTA3D = Boundary Layer code for Stability Analysis 3D, boundary layer profile solver
BWB = Blended Wing Body
CATNLF = Crossflow Attenuated Natural Laminar Flow
CCURV = Constrained CURVature, design constraint
CDISC = Constrained Direct Iterative Surface Curvature, design module
CODISC = Constrained, Optimization Direct Iterative Surface Curvature, optimization method
CF = Crossflow
CFD = Computational Fluid Dynamics
CRM = Common Research Model
CRM-M8 = Mach-0.8 variant of the Common Research Model
CRM-NLF = Common Research Model with Natural Laminar Flow
DEP = Distributed Electric Propulsion
DISC = Direct Iterative Surface Curvature
DLR = German Aerospace Center
HEC = High-End Computing
HSR = High-Speed Research program
HWB = Hybrid Wing Body
LaRC = Langley Research Center

[1] Senior Research Engineer, NASA Langley Research Center, Configuration Aerodynamics Branch, AIAA Associate Fellow.
[2] Research Aerospace Engineer, NASA Langley Research Center, Configuration Aerodynamics Branch, AIAA Member.
[3] Research Aerospace Engineer, NASA Langley Research Center, Configuration Aerodynamics Branch, AIAA Member.

JAXA = Japan Aerospace Exploration Agency
LASTRAC = Langley Stability and Transition Analysis Code, transition prediction software
LERAD = Leading-Edge RADius, design constraint
LST = Linear Stability Theory
MAC = Mean Aerodynamic Chord
MATTC = Modal Amplitude Tracking and Transition Computation, transition prediction software
NAS = NASA Advanced Supercomputing
NASA = National Aeronautics and Space Administration
NF = N-Factor
NLF = Natural Laminar Flow
NS = Navier-Stokes
NTF = National Transonic Facility
PAI = Propulsion-Airframe Integration
SCR = Successive Constraint Release
SETFP = SET Flow Parameter, design constraint
SETDP = SET Design Parameters, design constraint
SUE = Set-Up Executor code
SUSAN = SUbsonic Single Aft eNgine
TetrUSS = Tetrahedral Unstructured Software System, flow solver package
TCA = Terminal Configured Aircraft
TPGEN = Target Pressure GENeration, design constraint
TSD = Transonic Small-Disturbance
TS = Tollmien-Schlichting
TSD = Transonic Small-Disturbance
TTBW = Transonic Truss-Braced Wing
UCAV = Unmanned Combat Air Vehicle
UDF = Universal Damping Function
UEET = Ultra-Efficient Engine Technology program
USM3D = Unstructured Mesh 3D, Navier-Stokes flow solver
VSP = Vehicle Systems Program
VSTFE = Variable-Sweep Transition Flight Experiment

Symbols

α = Angle of attack, degree
c = Chord length, feet
c_f = Sectional skin friction coefficient, nondimensional
c_l = Sectional lift coefficient, nondimensional
c_m = Sectional pitching moment coefficient, nondimensional
C_L = Total vehicle lift coefficient, nondimensional
C_D = Total vehicle drag coefficient, nondimensional
C_m = Total vehicle pitching moment coefficient, nondimensional
C_P = Pressure coefficient, nondimensional
D = Drag, pound-force
L = Lift, pound-force
M = Mach number, nondimensional
M_n = Local Mach number normal to the shock, nondimensional
Re_θ = Reynolds number based on attachment line boundary layer momentum thickness, nondimensional
Re_c = Reynolds number based on local chord length, nondimensional
Re_{MAC} = Reynolds number based on mean aerodynamic chord, nondimensional
Re_T = Reynolds number based on transition location, nondimensional
$(r/c)_{LE}$ = Leading-edge radius, nondimensionalized by local chord
$(t/c)_{max}$ = Maximum airfoil thickness, nondimensionalized by local chord
x_1 = Location of beginning of rooftop pressure gradient, nondimensionalized by local chord
x_2 = Location of end of rooftop pressure gradient, nondimensionalized by local chord
x/c = x-location, nondimensionalized by local chord
y/c = y-location, nondimensionalized by local chord

$(x/c)_t$ = x-location of transition, nondimensionalized by local chord
η = Semispan location, nondimensionalized by semispan length
Λ_{LE} = Leading-edge sweep, degree
θ = Twist, degree

I. Introduction

IN July of 1973, the first AIAA Computational Fluid Dynamics (CFD) conference was held. According to Antony Jameson [1], one of the most noted CFD developers, this marked the beginning of CFD as an accepted tool in the aircraft design process. Papers published in 1998 [2] and 2003 [3] gave summaries of the tremendous progress in CFD methods for analysis and design, especially automated design codes, from the perspective of experienced industry designers. These papers mention the Constrained Direct Iterative Surface Curvature (CDISC) code as one of several design methods that helped to advance the state of the art in aircraft design. Twenty years later, the CDISC method has entered its fifth decade of use and continues to evolve to stay relevant as CFD and computer technology continues to progress. In the following subsections, the genesis and growth of CDISC, along with some examples of its application by NASA, industry, and others, will be given for each of these decades, according to the year the work was reported. A detailed description of the CDISC design philosophy and method, with some context relative to other design approaches, will be given in a subsequent section, followed by an example of its use in a preliminary design case.

II. History of Development and Applications

A. The 1980s – Seeing the Potential

For most of the 1980s, the flow solvers used in aircraft design were based on potential flow methods. These included the full-potential methods, such as the NYUH 2D airfoil code [4] and the 3D FLO codes of Jameson (e.g., FLO22 [5]), as well as the transonic small-disturbance (TSD) approach of Boppe (e.g., WBPPW [6]) and others. While the TSD method was a bit less accurate in theory, it allowed much more geometric complexity through the use of an embedded grid approach, modeling arbitrary fuselage shapes, as well as pylons, engines, and winglets. Regardless of the flow physics modeled, all of these codes had internal grid generation, with the geometry input as simple wing or fuselage cross-sections.

In the early 1980s, the first author had the opportunity to work with Dr. Michael Mann at NASA Langley Research Center (LaRC) on a design to improve the performance of a supercritical maneuvering fighter wing [7]. The design changes to the airfoils on the wing related surface curvature to pressure coefficient (C_P) based on a piston analogy and Prandtl-Meyer expansions for supersonic flow [8]. This approach was similar to that developed by Barger [9] and later improved upon by Davis [10], who used a hybrid algorithm that related C_P changes to airfoil slope in the supersonic region. Interestingly, while the use of the curvature-C_P relationship is technically valid only in the subsonic regions, both Barger and Mann were able to get good designs using it in the supercritical rooftop region as well.

In Mann's process, the surface curvatures and pressure coefficients were plotted by hand and changes to the airfoil coordinates were made by relating changes in C_P to changes in curvature. The modified airfoil coordinates were then inserted into the input file for the flow solver (FLO22, later updated to FLO27 [11]) for reanalysis. This cycle was continued until satisfactory wing pressure distributions were obtained. Though this design approach was successful in achieving improved wing pressures and performance, the manual process was very cumbersome and slow, so the first author decided to automate the change process and add this into an iterative loop built into the flow solver chosen for analysis. This automated process would eventually be named the Direct Iterative Surface Curvature (DISC) method and was first described in detail by Campbell [12].

The DISC method was used in several design projects in the mid 1980s, two of which were related to laminar flow. The first of these was the design of a natural laminar flow (NLF) wing for a transonic corporate transport [13]. As this configuration had low sweep, the design work was done in 2D, using the DISC method coupled with the NYUH flow solver. Evaluations of the initial and final wings were made using the WBPPW and TAWFIVE [14] codes and confirmed that the 2D design approach was adequate. Wind tunnel testing of the final airfoil confirmed that the desired characteristics were achieved.

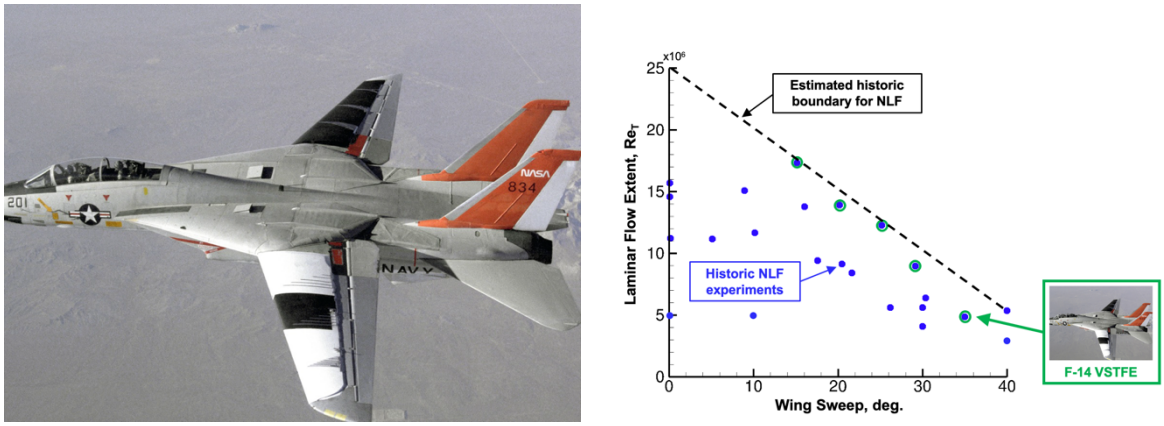

a) Test aircraft with NLF gloves. [Photo: NASA]

b) Glove 2 transition results.

Figure 1 – F-14 Variable-Sweep Transition Flight Experiment [15,16].

The second and more significant project involved the design of an NLF wing glove for the F-14 Variable-Sweep Transition Flight Experiment (VSTFE) [15]. As with the case above, because this design was to be done at the low-sweep condition (20 degrees), it was decided to use the NYUH code to generate the new airfoil sections, followed by 3D analysis of the wing modified with the new airfoils. In addition, considerable manual manipulation was required to fit the new airfoils smoothly onto the existing wing while maintaining glove thicknesses to meet structural and other constraints. The final 3D analysis using the TAWFIVE code indicated that the desired pressure architecture on the wing upper surface was achieved. This glove (referred to as glove 2) and a "clean up" glove (constant thickness overlay, glove 1) were added to the aircraft (see Fig. 1a). The aircraft was successfully flown in 1986-87 at a variety of speeds and altitudes, with wing sweep varying from 20 to 35 degrees. The results were reported in terms of extent of laminar flow (expressed as transition Reynolds number, Re_T) versus wing sweep angle varying from 20 to 35 degrees [16]. To date, the glove 2 data still has the highest transition Reynolds number for a given sweep in this range of any data in the publicly available literature of which we are aware (see figure 1b, data with green circles).

As the decade was ending, the DISC method was beginning to receive interest from industry, and codes with the design method installed began to be disseminated. At this time, the target pressures still needed to be externally generated for input into the codes. As noted in Ref. 8, some geometry constraints were beginning to be included, but not yet the common ones used in design. Also, each code had its own version of DISC installed internally in the code and consistent with the flow and geometry variables in that code. This would change in the next decade as the new Euler and Navier-Stokes codes gained acceptance.

B. The 1990s – Stoked by the New Flow Solvers

While Euler codes entered the CFD arena in the early 1980s, followed by Navier-Stokes (NS) codes towards the end of the decade, it was not until the early 1990s that they were used with DISC in automated design processes. One reason for the delay was that the potential flow codes with boundary layer included did a reasonable job of predicting the flow at cruise conditions and were much cheaper to run. Another reason for not shifting to the NS codes was that a direct coupling approach had been used with the potential flow codes, in which the DISC design module was built into the flow solver as subroutines, thus requiring access to the flow solver source code. In 1990, researchers at Boeing had developed an Euler code [17] and coupled it with the design module for what was likely the first example of 3D Euler design with DISC. Lin [18] reported doing successful designs for nacelles and a winglet with this code, noting rapid design times, but also noting that it required aerodynamic experience to define viable target pressures. The following year, Bell [19] at General Electric engines used DISC with an Euler version of the NASA CFL3D flow solver [20] to design the nacelle of a powered engine. In 1993, Chen [21] extended the earlier work of Lin to installed nacelles using DISC with an inhouse multiblock Euler solver, reporting effective design in about the same time as required for the baseline analysis. Also using Chen's Euler code, Wie [22] used DISC design to match the target pressures needed for a hybrid laminar flow nacelle.

The success of DISC design with Euler codes was followed by Boeing's interest in the NASA TLNS3D NS code [23], for which the source code was available, along with local support for its use. In 1992, Yu [24] reported on the

coupling of the DISC method with TLNS3D, showing wing design results from what was one of the first 3D NS design methods. Design times of 1-3 times the baseline analysis were reported, and it was noted that flow and geometry constraints would be a useful addition to the method. The following year, Shmilovich at McDonnell Douglas reported success using the new NS design method for wing design at cruise and buffet conditions [25]. In 1995, Jou at Boeing commented that DISC was one of the "inverse design methods which have revolutionized the transport airplane design process" [26].

While these NS designs were certainly encouraging, they were limited to the wing-body capability of the original TLNS3D code. Recognizing the need to analyze and design more realistic geometries, the flow solver was modified to use multiblock structured grids as was done with earlier Euler codes. These grids were no longer generated automatically within the flow solver, but were created with an external grid generation code and read as an input. This change prompted a modification to the design process, with the DISC module as a separate code run in a loop with the flow solver in a script. Flow and geometry information was passed between the two codes via auxiliary codes that used grid and flow files written in PLOT3D format [27], a new standard at that time. While this indirect coupling approach increased the design time slightly due to input/output overhead, it greatly increased the portability and maintainability of the design module. This change enabled a NS version of the CFL3D flow solver [28] to be easily coupled with DISC. While these grids did allow more geometric complexity, they could be difficult to generate and were often the bottleneck in the analysis and design process. The NASA Advanced Subsonic Transport (AST) Program that started in this time frame tried to address this issue by supporting the development of overset grids, with the NASA OVERFLOW NS code [29] as a prime example. Dr. Steven Krist at NASA LaRC coupled the DISC design module with this flow solver to create the OVERDISC design method. While this approach did simplify the grid generation process, it also required projecting changes made in one grid block onto other intersecting grid blocks. The first reported application of OVERDISC was in 1995 for the design of isolated and installed nacelles [30].

Several users had reported that, while the design method was fast and generally effective, it would be helpful if flow and geometry constraints were available. To address this request, a method was proposed by Campbell [31] that placed control points on the current analysis pressures, then adjusted their chordwise location and/or level, with linear changes in between control points, to directly meet flow constraints such as lift, pitching moment, or shock strength. Geometry constraints such as maximum or local thickness and leading-edge radius were indirectly addressed through empirical algorithms relating changes in C_P to changes in those geometric parameters (e.g., add negative C_P increments to target pressures on upper and lower surfaces to increase airfoil thickness). This approach was successfully demonstrated in 2D and included an early attempt at optimization called Successive Constraint Release (SCR). In this approach, a control point value, such as shock strength, could be set to a minimum value (e.g., shock Mach number = 1.0), then released to increase until all the other constraints were met. Although it is fairly simple, this approach that adjusts a constraint value based on a current flow variable, referred to as a "smart" constraint, is still in use today.

While the above method worked, it was decided that a couple of changes would simplify adding new constraints and take advantage of the previous experience gained in applying the DISC method. The first change was that the overall control point approach was abandoned. While some target pressure changes would still be made based on point locations and levels, others, such as lift and pitching moment, would use "shape functions" to make changes consistent with flow regimes or airfoil type (e.g., supercritical). Also, some flow constraints would create the whole target pressure architecture based on experience gained from recent design projects. An example would be a target pressure distribution for a supercritical airfoil at a given lift coefficient with a relatively flat supercritical rooftop ending in a weak shock and having significant aft loading. The second change was the use of direct geometry constraints, where the surface shape itself is changed to meet the constraint independent of the target pressures. The design process was then broken into 3 distinct parts: first it would loop through the flow constraints to try to define a target pressure that met all the constraints, then use the basic DISC algorithm to change the current geometry to try to match the targets, and finally apply the geometry constraints to the new design shape. This process gave the geometry constraints priority over the flow constraints, but typically after 20 or so design cycles the character of the flow constraints could be achieved while meeting the geometry requirements. This approach was documented by Campbell [32] with the code name changed to CDISC and included over 25 flow and geometry constraints. This general approach is still in use today.

The final years of the decade primarily involved applications of the CDISC method using the NASA NS flow solvers on configurations connected to the NASA AST and High-Speed Research (HSR) programs. As the AST program was focused on developing and transferring technology to industry for use in aircraft design, not all the work was reported in the general literature such as conference publications. One example of this was the application of OVERDISC to the proposed MD-XX transonic transport. The first author and fellow NASA researcher Dr.

Steven Krist spent multiple weeks onsite at McDonnell Douglas learning about their aircraft design process and helping them apply the OVERDISC method to their configuration, modifying the code as needed to make it more effective. The CDISC method was used effectively to improve performance at cruise while reducing buffet, with this design being the preferred configuration when the program was canceled upon their merger with Boeing. Some of the lessons learned from this experience were summarized by Campbell [33]. One of the key benefits of CDISC that became apparent in this project was the ability to design using the same flow solver and grid size that would be used for making final performance predictions.

Another configuration that received attention during the AST program and continued to develop afterwards was the Blended Wing Body (BWB) aircraft proposed by Liebeck [34]. Potsdam [35] was the first to publish design results on this configuration using CDISC coupled with CFL3D. He notes that the design successfully improved the performance of the aircraft and utilized a newly developed hard surface constraint, along with more typical geometry constraints, such as thickness. The hard surface constraint defined the region of the passenger compartment that the outer mold line could not penetrate. This was essential to this design since the entire body and wing area was subject to change to improve the aerodynamic performance. Also utilized was a new span load constraint that prescribed an elliptic load profile for minimum induced drag. Further BWB design using CDISC with CFL3D and OVERFLOW, with the latter used for full wing/nacelle design, is given by Liebeck [34].

In the HSR program, CDISC with TLNS3D was used in some of the early studies looking at wing/fuselage cases for the Terminal Configured Aircraft (TCA). Having less familiarity with the pressure distribution characteristics for efficient supersonic flight, this study was more about gaining a knowledge base from the results of the application of optimization methods by others. Some of the lessons learned were built into CDISC and applied to multipoint wing designs by Campbell [36] and for full configurations with engines by Krist [37].

Figure 2 – F-16-XL with laminar flow wing gloves. [Photo: NASA]

Also, under the HSR program was a proposed flight test to evaluate the feasibility of obtaining hybrid laminar flow on a F-16XL aircraft (see figure 2). Anders [38] gives an excellent review of the design of the wings for laminar flow as well as the testing procedure and results. He mentions that CDISC coupled with TLNS3D was used to design the wing to achieve the desired wing pressure distributions with a rapid acceleration near the leading edge and mild favorable gradient back to the expected transition location. Those pressure distributions were achieved in flight with significant extents of laminar flow obtained with suction. This example highlights one of the strengths of the CDISC method in its ability to design an airfoil or wing rapidly and accurately to a specified pressure distribution, a key requirement for natural or hybrid laminar flow designs.

One final change worth noting for this decade was the development of NS codes that utilize unstructured grids. This approach seemed to hold promise for greater ease of grid generation even in comparison to the overset grid approach. Two NASA codes, USM3D [39] and FUN3D [40], were developed in the mid 1990s, with Parikh [41]

doing the initial coupling of USM3D with CDISC in 1997. Although the unstructured nature of the grids made generation around complex configurations easier, it did introduce new difficulties in the process of extracting the flow information and modifying the surface and volume grids for reanalysis in the design loop, and those processes are still evolving, especially with the introduction of mixed-element grid flow solvers. Some results from CDISC coupled with USM3D on a business jet configuration with a pylon and nacelle are shown in Ref. 33, with an example of fuselage design to clean up adverse propulsion-airframe integration (PAI) effects. The USM3D/CDISC combination would eventually become the primary method used at NASA LaRC and would see significant use in industry as well. Regardless of whether it was this code pairing or OVERDISC, the design of complex configurations using NS solvers was becoming the norm.

C. The 2000s – More Application Than Development

As noted in Refs. 1-3, CFD analysis and design methods were an integral part of the aircraft design process by this time. Johnson [3] notes that CDISC combined with TLNS3D (Johnson refers to this code as A619) and OVERFLOW were not just research tools but were being used in the product development organization for configuration design. The CDISC method and the NASA flow solvers with which it was coupled were fairly stable developmentally and the focus during this decade was primarily on application. Design work initiated during the AST program continued for several configurations either within the companies or as part of new NASA programs such as the Vehicle Systems Program (VSP) and the Ultra-Efficient Engine Technology (UEET) Program. Even though the focus tended to be on application, the new configurations brought new challenges that required some extensions to the design method.

One AST related project that was reported by Olsen [42] was the design of a wing using OVERDISC for a wind tunnel test. The goal of this design was to produce a wing with a specific pattern of shock-induced separation leading to cruise buffet to provide data for the validation of CFD turbulence models at these conditions. The wind tunnel test confirmed that the design had the desired progression of separation and provided several types of data for assessing the turbulence models. Work on the BWB that began during the AST program also continued, with Roman [43] giving a nice summary of the design work to date using CFL3D and CDISC to improve the performance through a series of designs. In a design that explored pushing the BWB toward higher cruise speeds, Roman [44] was able to develop a configuration with a drag divergence Mach number slightly above 0.93, citing the ability of CDISC to produce “weakened shocks and less aggressive trailing edge pressure recoveries”, while also meeting a number of flow and geometry constraints. Roman notes that CDISC with CFL3D “proved to be an extremely valuable tool for BWB clean wing design”.

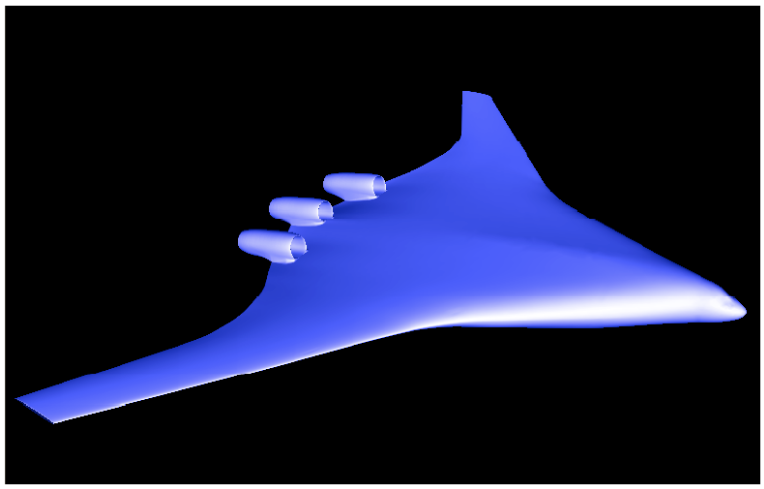

Figure 3 – Blended Wing Body with BLI nacelles. Graphic from [45].

While much of the BWB design work cited above was done without nacelles installed, analysis and design cases of the aircraft with various propulsion systems, including mail-slot and individual engine boundary-layer ingestion (BLI) approaches as well as more conventional pylon-mounted engines, were carried out during and after the AST program. An example of a design to improve the propulsion-airframe integration for a configuration with 3 individual BLI engines mounted on the aft upper surface (see figure 3) is given by Campbell [45]. An earlier

unpublished design used OVERDISC to modify the outer nacelle shapes for a twin-engine BLI configuration. While this design nearly eliminated PAI-related shocks and increased lift-to-drag ratio (L/D) by 6.5%, grid movement difficulties at the nacelle-wing intersection dictated that this region remained fixed. To try to alleviate this problem, it was decided to use USM3D for the three-engine case to see if the unstructured grid gave more design freedom at the wing/nacelle interface. Also, CDISC with USM3D had a zonal design capability, where a subset of the full grid and initial flow solution could be extracted, and local design continued with the flow "frozen" at the boundaries of the extracted region. The final design zonal grid could then be plugged back into the full grid for final analysis. This approach has saved significant time for small or partial component designs on several configurations.

The BWB baseline flow analysis indicated some weak-to-moderate shocks on the nacelles that contributed to flow separation ahead of and in the duct that also spilled around the nacelles and contaminated the elevon between the engines. The CDISC design automatically toed the nacelles to provide better alignment with the approaching flow and modified the ramp ahead of and into the duct to significantly clean up the separation in that region as well as near the elevon trailing edge. The baseline and designed surfaces were built and tested in the National Transonic Facility (NTF) at NASA LaRC, with the experimental results confirming the predicted changes in drag as well as flow direction changes.

A second major application of CDISC during the 2000s was the High-Speed Slotted Wing configuration, a cooperative project with Boeing under the NASA VSP portfolio [46]. This technology was first developed by Whitcomb [47] in the 1960s and involves a slot between a main airfoil element and aft flap at cruise that allows more aft loading on the airfoil without separation, thus producing lower supercritical rooftops and weaker shocks for a given lift. The performance of these airfoils was highly dependent on the slot flow and the interaction between the elements, but CFD was still in its infancy at that time and could provide little guidance for design. Whitcomb therefore chose to abandon the slotted airfoil work and focused on the more robust but slightly poorer performing supercritical airfoil.

Significant improvements in 3D CFD analysis and design capabilities were made in the 30 years or so following Whitcomb's decision, leading Boeing to revisit the cruise slotted wing technology as a potential candidate for the B787 aircraft then in design. Several teams of Boeing and NASA researchers were formed that used OVERDISC as well as the TRANAIR optimization code [48] to design wind tunnel models to assess the slotted airfoil technology, mainly in the context of increasing the cruise speed of a twin-aisle aircraft. From a CDISC perspective, it required the development of several new constraints, including ones that addressed the additional design space created by the location and orientation of the two elements (e.g., gap, overhang, and flap deflection). Over several years, many designs were made with both methods, several of which resulted in wind tunnel models. The tests of these models confirmed the predicted cruise speed increase, but some of the details of the flow in the slot region were still not accurately computed. Though other evaluations of the wings related to high-lift and flutter were made and gave encouraging results, the technology was deemed not mature enough for the B787 and further research was paused. However, the work was successful enough that two patents were obtained based on the research efforts [49,50]. The NASA Advanced Air Transport Technology is currently revisiting the concept for a generic single-aisle aircraft and will be described in a later subsection.

Several other design projects were done with CDISC that were smaller in scope but demonstrate the breadth of application of the method. A Mars Flyer configuration was designed with the plan of having it fly in the Martian atmosphere in 2003, the 100th anniversary of the Wright brothers first flight. The challenge of this design was trying to provide significant lift at transonic speeds at a chord Reynolds number of 40 thousand. The design relied on a newly developed "second leading edge" boundary layer tripping technique to reattach the separation bubble that occurred at the high design-lift coefficient. Though the project was ultimately cancelled, several wind tunnel tests [51] indicated that the design was successful.

Under the NASA Morphing project, a flow control concept using active contour bumps to control wave drag and flow separation increases at off design conditions, required design of the bump shapes at multiple design points [52]. A new constraint that created a bump and adjusted its height based on the local flow conditions was added to CDISC and evaluated using the MSES 2D code to design a family of bump shapes at different flow conditions. Wind tunnel testing of the bump shapes indicated significant drag reduction at the higher lift conditions as predicted [53].

Some CDISC work was also done at higher speeds. A renewed interest in making supersonic transport flight viable by reducing sonic boom levels to allow overland flight led to projects such as the NASA Shaped Sonic Boom Demonstration flight and Gulfstream's Quiet Spike. NASA worked with Gulfstream on supersonic wing design to look at both performance and boom metrics, but the proprietary nature of the work kept it from being published.

A final example at even higher speeds is an exploratory study of the use of CDISC to design blunt bodies at hypersonic speeds [54]. This required a change to the fundamental DISC algorithm relating shape change to a desired flow change, where a modified Newtonian theory was used for the windward side, then automatically

switched to the standard supersonic algorithm on the leeward side. A surface heat transfer constraint was added, and the final process was run with the OVERFLOW code on 2D blunt body configurations. The design process was generally successful, though heating loads tended to be redistributed rather than alleviated.

D. The 2010s – New Transitions to NLF and Optimization

The new decade would bring somewhat of a shift from close interaction with industry to more focus on design projects within NASA and some international cooperative efforts. NASA had set several ambitious goals in their Subsonic Transport System Level Metrics, including a 60% reduction in fuel burn by 2025 [55]. Reaching this goal would require more efficient airframe concepts, such as the BWB and the Transonic Truss-Braced Wing (TTBW), as well as individual technologies, such as laminar flow and active flow control. The CDISC design method would play a significant role in both approaches.

One of the major themes of CDISC development and application during this time was natural laminar flow (NLF), which was also the subject of several design studies using the earliest versions of the code. The CDISC method is especially well suited to laminar flow design since it efficiently drives surface pressures toward a specified target distribution, which is the key factor in controlling the growth of disturbances in the boundary layer that lead to transition. Early in the decade, NASA and the German research agency Deutsches Zentrum für Luft- und Raumfahrt (DLR) established a cooperative agreement to look at NLF analysis and design methods. As DLR had a design method similar to CDISC that designed to target pressures, one of the goals of the research was the development of a method [56] that could optimize NLF target pressure distributions by balancing extent of laminar flow with profile and wave drag. The values of the various drag components were estimated from some empirical rules developed from 2D parametric studies and a simplified method for estimating transition location based on Tollmien-Schlichting (TS) and crossflow (CF) growth, referred to as MATTC, and an assumed critical N-factor value. The method was successfully applied to a transonic airfoil design and components of this approach were later built directly into the CDISC code.

While the emphasis during the work with DLR was on controlling TS growth to allow a given extent of NLF, some ideas for suppressing the rapid CF growth near the leading edge of a swept wing were also explored. These ideas were further developed, along with a function for tailoring TS growth referred to as the universal damping function (UDF), and both approaches were incorporated into CDISC. Two design efforts, both using the USM3D flow solver, were then undertaken to test the new design approach, which would eventually be referred to as Crossflow Attenuated NLF, or CATNLF.

The first of these studies was done through an international cooperative agreement with the Japanese Aerospace Exploration Agency (JAXA), looking at trying to get NLF on a Concorde-sized supersonic transport. Each organization applied their own design method, flow solver, and boundary layer stability analysis codes to the problem. For this configuration, NASA used the CART3D Euler code [57] with CDISC for the initial design work as it was very fast and viscous effects were not as significant as in a transonic design with supercritical airfoils. The USM3D NS code was used to finalize the design and compute the drag savings for the laminar versus turbulent flow cases. Despite some differences in final shapes due to differing geometry constraints, both NASA and JAXA achieved similar extents of NLF [58], further verified by cross-analysis of the final geometries. The details of the NASA design are given in Ref. 59 including a reduction in wing/body drag of about 5% and transition Reynolds numbers as high as 36 million on a wing with leading edge sweep as high as 72 degrees. It should be noted that while both NASA and JAXA designs showed significant laminar flow, the critical N-factor that was used was 13 for all computations. While this value was based on several reported flight experiments, it is dependent on the stability analysis assumptions and was likely too high.

A second major series of NLF designs began with an in-house exploratory application of the methodology developed during the supersonic study to a generic transonic transport, the Common Research Model (CRM) [60]. Though the wing leading edge sweep (37 deg) and Reynolds number based on the mean aerodynamic chord (30 million) were considerably lower for this configuration compared to the one used in the work with JAXA, the higher relative wing thicknesses and sectional lift coefficients added to the difficulty of achieving large extents of laminar flow, especially inboard on the wing. As reported in Ref. 61, a successful design was achieved for a critical N-factor value of 13, the same as used in the supersonic study with JAXA. Also included in that report was an initial look at an NLF design of the CRM for testing in the NTF. While the tunnel is capable of testing at flight Reynolds numbers, the freestream disturbance levels are higher than would be seen in flight. An NLF test by Crouch [62] in the NTF suggests that a critical N-factor of 6 is more representative of that tunnel's environment. The attempted design using this critical N-factor was successful at reducing TS levels to allow large runs of laminar flow, but the leading-edge CF peak could not be brought down to the required level.

Several modifications were made to CDISC as a result of the wind tunnel model study, including a new shape change algorithm applied only in the leading-edge region to provide a better match to the rapid acceleration in the target pressures in that area required for CF peak suppression. In addition, a planform geometry constraint was added that automatically reduces wing sweep near the root to reduce Re_θ values there below 100 to prevent attachment line contamination from the fuselage boundary layer. This reduction in sweep was also beneficial in suppressing the CF peak in that region. The changes in the design method are described in Ref. 63, with details on the design of the new model, designated CRM-NLF, reported in Ref. 64. The model was built and tested in the NTF (see figure 4), with results and post-test analysis reported by Lynde [65,66]. The test was generally successful, though the occurrence of turbulent wedges on the wing due to particulates in the tunnel freestream limited the useful data at higher Reynolds numbers. The CATNLF design approach in CDISC was successful at suppressing CF peaks at Reynolds numbers based on mean aerodynamic chord as high as 22 million and achieved a transition Reynolds number of 10 million at a leading-edge sweep of 37 degrees, about double the maximum reported in the literature previously. The geometry and data from this test were used as the primary test case for the first AIAA Transition Modeling Workshop in 2021.

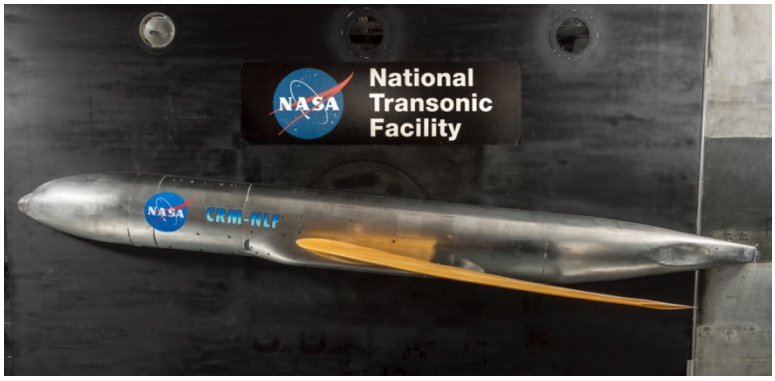

Figure 4 – CRM-NLF semispan model in the NTF. [Photo: NASA].

Another key area of expansion of CDISC design during the 2010s came about in the context of Air Force interest in improving the utility and performance, including speed, of the military transport fleet. Zeune [67] reported on work done by AFRL, NASA, and industry to accomplish these goals that included new configurations as well as technologies such as active flow control. One of the industry participants utilized CDISC and a sister code, SUSIE, to design the TEMPO configuration for increased speed and efficiency, with NASA modifying the design codes to meet new geometry constraints as well as facilitating use with circulation control. To improve the selection of CDISC flow constraint input parameters from both an effectiveness and time metric, Hooker [68] reported that an optimizer loop was wrapped around CDISC and SUSIE, with the resulting system, KNOPTER, being 3 to 5 times faster than designer-in-the-loop changes. Using this approach in their final detailed design showed an increase in cruise Mach number from 0.77 to 0.81 and a 15% improvement in ML/D relative to their preliminary design starting point and 43% relative to the initial conceptual design.

The KNOPTER system was later successfully applied to the Over Wing Nacelle [69] and Integrated Distributed Propulsion [70] configurations, with the wing redesigned for each propulsor concept and location, requiring thousands of NS flow analyses for design. This highlights the speed of the CDISC method in producing a design in about the same time as a converged analysis-only run. Another application of the KNOPTER/CDISC design method was to a new transport/tanker concept, shown in figure 5, referred to as the Hybrid Wing Body [71]. This configuration offered dramatic improvements in fuel burn relative to the C-17 fleet and even some improvement relative to modern commercial transports, which drew interest from NASA. The designs included clean wing as well as a multitude of propulsion/airframe integration cases for different engine types, requiring more that 10 thousand runs of the USM3D NS code for both analysis and design. The configuration was tested in the NTF [72,73], with the results confirming the predicted efficiency of the HWB concept as well as benefits of the over wing nacelle installation.

Figure 5 – KNOPTER/CDISC designed Hybrid Wing Body in the NTF. [Photo: NASA from Ref. 73].

While optimization using the CDISC flow constraints had been used before for simple demonstration cases, the general approach to CDISC is to build rules into the constraints that would yield a near-optimum design with off-design performance taken into consideration. The success of the KNOPTER approach prompted a new look at simple optimization to improve performance within this framework of multipoint thinking. The CODISC method [74] was therefore developed to explore improving the effectiveness of CDISC with minimal impact on efficiency. For this study, a separate code (SOUP) was developed to read the global lift and drag coefficients from the flow solution, adjust the constraint variables in the CDISC input file, and control the overall design convergence process. Several design examples involving both transonic and supersonic flow were included, with a standard CDISC design used to improve the baseline performance before using CODISC. In each case, a simple global variable was used to vary the spanwise distribution of the UDF rooftop pressure gradient parameter with the goal of minimizing drag while maintaining the design lift. All the examples showed additional drag reductions beyond the simple CDISC design and only took about twice as much time as the original design. While the method worked well, it was decided that the final spanwise distribution of UDF could be used to prescribe initial default settings for that parameter in the CDISC input file. Then, during the design, "smart constraints" that were built into CDISC could automatically adjust constraint parameters based on local flow variables such as shock strength and skin friction levels. It was thought that this approach might be a more efficient way to improve effectiveness as it does not require high levels of flow solution convergence.

The CDISC method was also utilized in the design of several wind tunnel models used in NASA programs during this decade. One was the design of a single-aisle transport with ultra-high bypass engines on pylons under the wing [75]. The CART3D-Adjoint Optimization Framework was used to do an integrated design of the wing and nacelle to improve the span load, reduce the strength of shocks, and eliminate double shocks. The optimization generally achieved these goals, but when the configuration was analyzed in the USM3D NS flow solver, the desired span-load and pressure distributions were no longer present. This was caused by the absence of viscous effects in CART3D (an Euler code) which are important for supercritical wings with significant aft camber. CDISC coupled with USM3D was used to redesign the final wing geometry so that the desired flow characteristics were recovered. This emphasizes the importance of being able to design with the same flow solver, or at least one that includes the needed level of flow physics, that is used for final analysis.

Another NASA wind tunnel model designed with CDISC and USM3D is the FAST-MAC model, a generic supercritical wing/body semispan configuration with internal ducting to supply high-pressure air for flow control experiments [76]. The model was used throughout the decade looking at the effects of blowing through slots [77,78] with steady and sweeping jets [79,80]. CDISC was also used to design one of five candidate wing geometries for the Juncture Flow Experiment [81] utilizing a new flow constraint that modified target pressures to achieve a specified skin friction coefficient distribution. The five wings were tested in several wind tunnels to down select to a single

geometry for the final test, the results of which would be used to evaluate various CFD turbulence models for predicting side-of-body separation (the CDISC wing was not selected). In addition to wind tunnel models, CDISC was also used in the design of the cruise airfoil shapes for a couple of NASA distributed electric propulsion (DEP) test aircraft, the X-57 Maxwell [82] and the GL-10 Greased Lightning [83].

Two final design cases from this decade will be mentioned because of some design constraint developments that were unique and are still relevant today. The first is the design of a generic TTBW as part of the PADRI 2017 workshop [84], with the objective of reducing the shocks and flow separation between the wing and strut in the mid-wing region where they join, subject to thickness and other geometry constraints. Existing flow and geometry constraints were first applied and significant cleanup of the flow with the associated drag reduction was achieved. Based on the results of this design, a new constraint was added to specifically address the channel flow seen between the wing and strut. It is based solely on the geometry of the two components (wing and strut airfoil sections), creates a relatively flat-sided channel with a specified separation between the components, and requires no target pressures. Because of this, it is a "one-shot" design, only requiring one design cycle, but enough flow iterations in that cycle to converge the solution. This reduced the design time to about 25% of a converged baseline analysis, instead of the more typical factor of 1-2x for a normal CDISC design. As a point of reference on the effectiveness of these designs, both the standard CDISC and one-shot cases had almost identical drag reductions compared with results from numerical optimization [85].

The second case that required a significant change to the CDISC design process involved a supersonic configuration with the objective of modifying the near-field sonic boom signature, ultimately leading to reduced boom levels on the ground [86]. Normally, the CDISC design method changes a surface shape based on the difference between target and analysis pressures on that surface. In this case, the relevant pressures are in the flow field over a body length away from the surface, so a remote design capability based on ray tracing along Mach lines was developed. As a test of this method, a target pressure distribution was generated by running the LM1021 supersonic transport full configuration (i.e., wing/body/tail/engines) and extracting the near-field boom signature below the aircraft. This signature was scaled to match the length of the baseline for the design test, the SEEB body of revolution. The diameter of the SEEB body was then changed along its length based on the difference between the analysis and target pressures at the near-field cutting location 1.2 body lengths below the centerline of the body, with the standard CDISC design algorithm used to make the geometry changes. The remote design approach was able to match the complex waveform of the target signature very closely, a surprising result given the complexity of the aircraft geometry that generated the targets.

E. The 2020s – Still Pushing the Boundaries

During the last two decades, USM3D had become the primary flow solver used for our in-house designs as well as for some outside users. Other than some minor changes, such as adding an arbitrary transition location specification for laminar flow cases, the flow solver had remained largely unchanged relative to its fitting into the CDISC design process. The CDISC auxiliary codes used to couple the flow solver to the design module were developed based on the triangulated surface grid and tetrahedral cell volume grid used by USM3D. Toward the end of last decade, however, a new version of the flow solver, USM3D-ME [87], came out with significant changes. The code was significantly faster than the previous version but required the use of mixed-element grids to realize this improved performance. While some designs during the first couple of years of the current decade were done with the old code and grids, it was decided to completely re-write the CDISC auxiliary codes. In addition to reading and writing the new grid format and element types, the biggest change involved modifying the volume grid movement coding to move and clean up the non-tetrahedral cells as needed. A new version of CDISC was created as well to incorporate the recent lessons learned for robustness, effectiveness, and ease of use, as well as to remove old coding that had accumulated through the decades and that was no longer used. A description of some of the new code approach and methods will be given in the following section.

The primary in-house focus of CDISC application during the current decade has continued to be NLF design for transonic transport configurations. While the CRM-NLF wind tunnel test demonstrated that the CATNLF design approach in CDISC was generally valid, its potential was not fully explored due to limitations associated with the tunnel environment and model scale. This led to a proposal to design a partial wing for mounting under an F-15 for flight tests at NASA Armstrong Flight Research Center. Details of the design are given by Lynde [88] and an illustration of the test article, known as "Stubby", mounted under the aircraft is shown in figure 6. Though the partial

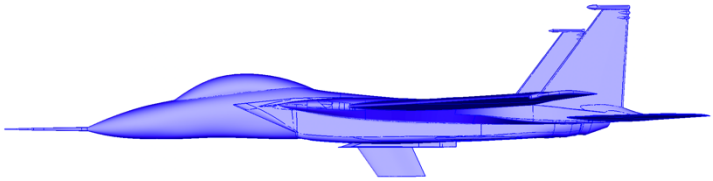

Figure 6 – CATNLF stub wing mounted under the F-15 test aircraft.[Graphic from [88].

wing appears simple, the design required trying to simulate flow typical of a transport wing with significant loading. The small aspect ratio meant that root and tip effects were evident across the whole wing. Mitigating these effects while meeting the CATNLF target pressures and Re_θ limits required both planform and airfoil changes. In addition to the goal of demonstrating that NLF can be achieved on a wing with sweep and Reynolds number representative of a single-aisle transport, the design includes features that should assist the transition modeling community in assessing their models in CFD codes. The test article has been built and is currently slated for testing in early 2024. If successful, the wing will have over 4x the extent of laminar flow in terms of transition Reynolds number, as the F-14 VSTFE data at the same sweep (35 degrees) as shown in figure 7.

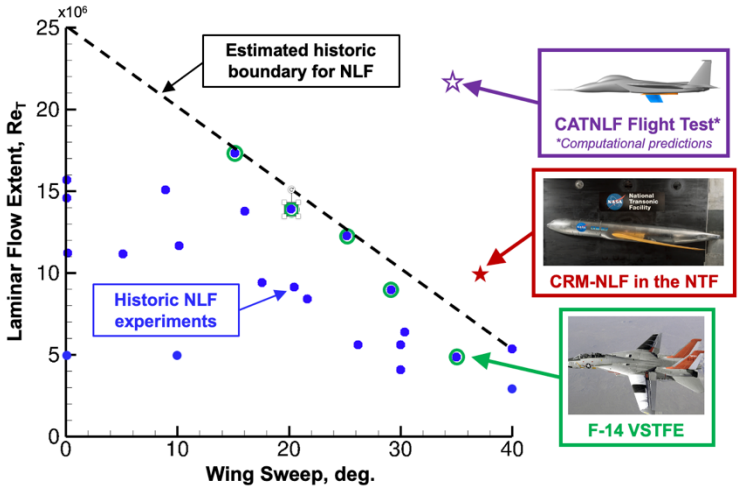

Figure 7 – CDISC NLF designs in perspective.

The test article was designed in the presence of the F-15, and its achievement of NLF is strongly dependent on the flow field of the aircraft. While the flight data will be of interest to aircraft designers as far as assessing the CATNLF method, it would be of limited use to the transition modeling community as the release of the geometry of the aircraft is restricted. To try to address this limitation, Banchy (formerly Lynde) [89] initiated a unique remote design using CDISC. For this case, a surrogate surface that creates a flow field similar to the F-15 was designed starting from a flat surface above the test article that replaces the whole aircraft. Initial target pressures for this design, known as the Equivalent Loading via Interference Surface Effects (ELISE), were developed from cuts through the flow solution on the lower surface of the F-15, then modified based on how well the pressures on the test article were matching the ones with the aircraft present. The process created two large bumps on the ELISE surface, with the resulting test article pressures matching very closely with the desired values.

Another case that used the CATNLF method in CDISC involved revisiting the concept of the High-Speed Slotted Wing (now referred to as a cruise slotted wing or CSW). Hiller [90] looked at applying the CSW technology to a modified version of the CRM that represents a single-aisle transport with a cruise Mach number of 0.8, known as the CRM-M8. In previous research with Boeing in the early 2000s, it was noted that the CSW had a skin friction drag penalty relative to a conventional wing. Though some of this penalty is associated with the extra wetted area in the slot, most of it appears to be related to the higher skin friction coefficients associated with the new, low-

Reynolds number boundary layer on the flap. It was proposed to design the flap using CDISC to have laminar flow on the upper and possibly lower surface of the flap in a concept known as Aft Laminar Multielement Airfoil (ALMA). A new series of flow and geometry constraints were developed to shape and position the two elements. Using these new constraints, a 2D ALMA airfoil was designed that had lower drag at cruise relative to a conventional airfoil and maintained an advantage across a range of near-cruise off-design conditions. This revised CDISC method is currently being applied to a 3D design of the CRM-M8 with both conventional and partial-span CSW wing configurations using the new USM3D-ME/CDISC combination [91]. Results so far indicate that the ALMA wing has cruise drag performance comparable to the conventional wing, but with improved drag divergence characteristics. Future work is planned to apply the CATNLF approach to design the main element of the CRM-M8 ALMA wing for NLF on the upper surface for additional drag reduction.

One of the primary uses for CDISC over the last decade has been to provide significant improvements to preliminary designs through the use of a few simple constraints with default values. This was the approach taken by Lynde in the design of the SUbsonic Single Aft eNgine (SUSAN) Electrofan configuration [92]. The baseline wing was taken from a similar configuration that had been designed using optimization, but when used for the SUSAN configuration at its cruise conditions, the wing produced multiple shocks and significant wave drag. Using the standard CDISC wing design constraint set, a new turbulent baseline wing was designed with much weaker shocks, and then the CATNLF approach was used to design a laminar wing to provide an accurate estimate of NLF benefit for use in systems analysis. The results indicate laminar flow could be achieved over more than half of the upper surface of the wing, providing a drag reduction of almost 9% relative to a well-designed turbulent baseline and maintaining an advantage across near-cruise off-design conditions. Note that the relative drag reduction is for a wing/body configuration and would be lower for the full aircraft.

In an effort to minimize drag for the full SUSAN configuration, a study was launched to apply CATNLF to the vertical and horizontal tails of that aircraft. The primary difference between using CATNLF on a wing and tail surface is related to the attachment line location. For a wing, the attachment line is typically on the lower surface such that the flow will travel around the high-curvature leading edge, which helps accelerate the flow rapidly, creating the key feature in attenuating crossflow growth. However, the horizontal tail lift at cruise is typically negative and lower in magnitude than for a wing, moving the attachment line much closer to the leading edge. Fortunately, the lower lift also means less acceleration is required and Pomeroy [93] reports that NLF was achieved as far back as $x/c = 0.65$ on the horizontal tail lower surface at the design stations. The vertical tail at cruise has the attachment line on the leading edge, thus providing no additional acceleration. This case required the development of a new CDISC constraint to keep the airfoil sections symmetric and automatically adjust the initial acceleration level to develop target pressures that would suppress the CF growth below the critical N-factor. The design at cruise conditions was successful, achieving laminar flow back to about $x/c = 0.4$ on each side of the vertical tail at the design stations, but generating atypical airfoil shapes to do so. Off-design analysis at near-cruise conditions is underway and assessment at take-off and landing conditions, where tail effectiveness is crucial, is planned.

One final area of laminar flow design is a revisiting of supersonic NLF in light of the interest generated by the NASA X-59 Low Boom Flight Demonstrator [94]. Following on the encouraging results from the earlier work with JAXA, Bozeman [95] has initiated a study looking at an early version [96] of the wing from the X-59 to examine the compatibility of low-boom with an NLF wing design. Some difficulties with movement of the mixed-element grid cells after surface modification for the complete configuration led to the initial design work being done on a wing-only configuration. This provided a means of checking the new CDISC code for supersonic design as well as assessing a new process for computing the transition location based on balancing the growth of multiple instability modes. The preliminary results look good, achieving a drag reduction of 8% for the wing alone. Work continues resolving the grid movement issue, as the boom level is strongly dependent on the full configuration.

A couple of advanced configurations in which CDISC played a role in the development were recently selected for large-scale demonstrator programs. Boeing was recently selected to build the NASA-sponsored Sustainable Flight Demonstrator [97] using their TTBW concept. In addition to other design codes, CDISC was used in the development of the predecessor SUGAR TTBW aircraft to reduce shock strength on both the wing and the strut, especially in the channel near the wing/strut juncture [98]. Also, CDISC was used to advance the design of a similar in-house version of a TTBW developed by system analysis researchers at NASA LaRC for use in evaluating various technologies. In another large demonstrator program, the Air Force selected a team headed by Jet Zero to further develop the BWB concept as a potential transport for troops and cargo [99]. The use of CDISC in the early development and maturation of the BWB concept over several decades was described in earlier parts of this section.

Finally, two CDISC designs involving military configurations were completed. The first was done by Banchy (unpublished) on a BWB-type configuration developed within the NATO STO AVT-298 task group for research on low-speed stability and control that would benefit UCAV as well as commercial or military BWB aircraft. The

original configuration did not have transonic performance typical of a BWB aircraft, so CDISC/USM3D was used to improve the configuration, lowering its cruise drag by 15% relative to the original baseline. A wind tunnel model of this final configuration was built and completed testing in the NTF earlier this year to provide a database for assessing how best to run CFD to predict the flow characteristics of interest. Publication of the design and test results, along with an extensive set of CFD predictions, is planned for next year.

The second military configuration design was done for a generic tailless fighter configuration by Weston [100] using the old versions of USM3D and CDISC. This is the first published fighter wing design using CDISC that the authors are aware of and, interestingly, comes full circle back to the work of Mann [7] that kicked off the development of CDISC over 40 years ago. The design successfully met the project objectives, reducing drag by over 11% at the cruise point design conditions and showing improvement across a range of near-cruise Mach numbers. Weston also comments that the total computational cost was very low, but it took some time to learn the CDISC process. As a new user from outside of NASA and with no formal cooperative program that would lead to more extensive interaction with the authors, Weston's experience and comments about the strengths and weaknesses of the old CDISC design process were extremely helpful toward development of the new process.

F. Lessons Learned

In looking at the successes, failures, and changes of CDISC over the last 40 years, several factors were identified as contributing to its longevity. The first and probably dominant reason for its acceptance and continued use was that it offered a practical design option for some popular flow solvers (TLNS3D, CFL3D, OVERFLOW, USM3D). As with CDISC, these NASA codes were available at no cost, and they were at the forefront of CFD development and often used to do the final performance analysis. None of these codes had companion adjoint solvers for determining sensitivity derivatives at the time of the coupling with CDISC, so the efficiency of CDISC design would have been at least two orders of magnitude better than a finite difference or search algorithm approach to optimization for wing design using these codes. Another factor was that CDISC was not just fast, but was generally effective at obtaining significant aerodynamic benefits, often giving improvements comparable to optimization when both methods were applied to the same case. The caveat here was that the design had to be within the knowledge base of CDISC, but this base can usually be built quickly using parametric studies, often using simpler cases like 2D airfoil studies. Finally, the CDISC approach of automatically generating target pressures to achieve the aerodynamic objective based on familiar engineering quantities like sectional lift and pitching moment coefficients, and similar airfoil geometric parameters such as thickness and leading-edge radius, made it easy to use, especially for experienced aerodynamicists that were used to evaluating wing pressure distributions. A discussion about efforts being made to maintain and improve upon the three Es of a good design method – Effectiveness, Efficiency, Ease of use - in the new code is given in the following section.

III. Method

The CDISC method is a knowledge-based approach to design that uses a set of rules to modify the geometry of an aerodynamic surface to try to obtain a desired flow characteristic. It is like an inverse method in that a flow quantity (typically a target pressure distribution at a design station) is the input, and the geometry (new airfoil or surface shape) is the output. However, CDISC does not use a switching of the dependent and independent variables to solve the inverse problem as with formal inverse methods. Instead, it uses a direct-iterative approach similar to optimization methods where a new geometry determined by the design algorithm is reanalyzed in the flow solver. This process is shown in the flow chart in figure 8, where the geometry and flow solution from the current flow solver run is read by an auxiliary code to extract the surface coordinates and flow variables at the design stations. This information is fed to the CDISC design module which will modify the geometry at the design stations based on the flow and geometry constraints. The new geometry is then passed to the grid modification module, where the changes relative to the baseline geometry are computed and used to modify the surface grid and then the volume grid, with any negative volume or badly distorted cells that were created by the grid movement process cleaned up. The final grid is then sent back to the flow solver where analysis is continued from the previous solution for the next design cycle. For a typical design, about 50 design cycles are required, with a total design time on the same order as the time for a converged analysis of the baseline.

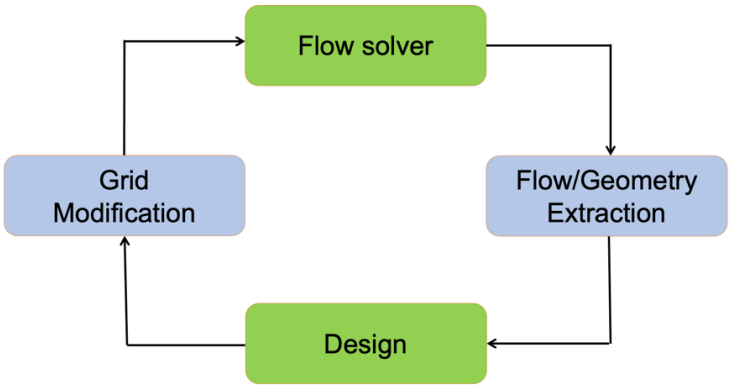

Figure 8 – Flow chart of CDISC design process.

A. Effectiveness

A design method must be able to give a significant improvement in a reasonable amount of time, including set up, run, and post-design analysis time, or it will not continue to be used (unless it is the only option). For a knowledge-based aerodynamic design method to be effective, the knowledge base must contain answers to the following three questions:

1) What flow physics relate to the desired aerodynamic improvement?
2) How can a flow characteristic (e.g., target pressure distribution) be specified to change the flow physics?
3) How can the geometry be changed to obtain the desired flow characteristic?

The most common aerodynamic improvement goal that CDISC is applied to is drag reduction, but it has also been used to address a variety of other objectives such as increasing maximum lift, reducing cruise buffet, and reducing sonic boom. Some of the flow physics associated with these goals are shocks, boundary layer state (laminar/turbulent, attached/separated), and vorticity. To illustrate how CDISC uses the knowledge-based approach, an example of cruise drag reduction for a transonic transport wing is given below, with the CDISC approach and limiting factors included for addressing each of the relevant components of drag and the related flow physics.

The TPGEN flow constraint is the primary method of automatically defining good target pressure distributions for drag reduction for a wing-like component (e.g., wing, winglet, tail, canard). It starts from the current analysis pressure distribution and modifies the pressures based on specified or computed values of the constraint input variables (see figure 9, turbulent case), along with the desired values of sectional lift and pitching moment coefficients, if specified. Three key parameters are used to build the rooftop architecture of the upper surface target pressures over the front of the airfoil: the locations of the beginning (x1) and end (x2) of the rooftop, and the value of the UDF parameter that controls the rooftop pressure gradient between these two points. A rapid acceleration is defined to connect the current analysis pressure coefficient at the leading edge to the initial target level at x1, and the pressures aft of the shock at x2 are adjusted to blend smoothly into the existing analysis values over the remainder of the upper surface. The desired lift coefficient is obtained by translating the rooftop up or down, with the pitching-moment adjusted toward a target value using a function that provides the aft loading commonly seen in supercritical airfoils. The values of x1, x2, and UDF can be input manually, but they can also be automatically set internally to default values determined from the CDISC knowledge base.

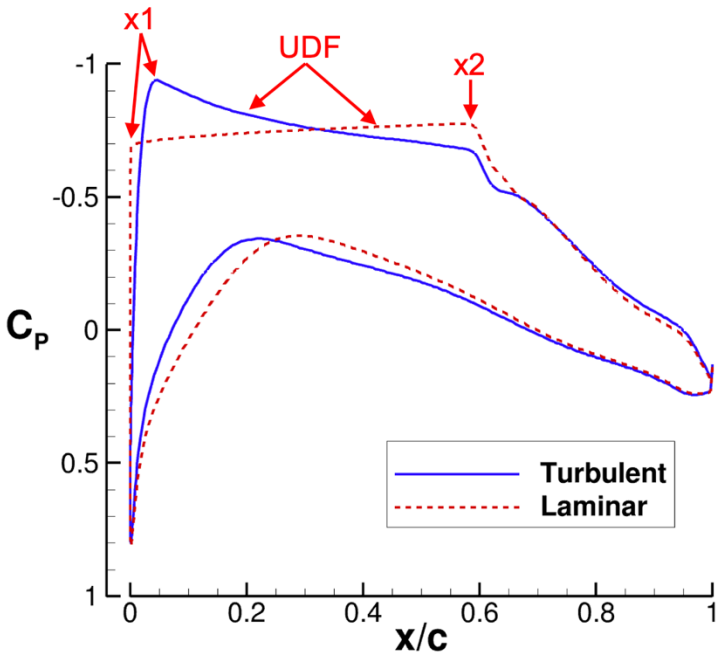

Figure 9 – TPGEN rooftop pressure input variables.

The first component of drag considered is induced drag. This is primarily related to the shed vorticity from the wing and, to a lesser degree, other lifting surfaces. The shed vorticity from the wing is set by the spanload distribution across the wing, with a theoretical minimum for a planar wing being an elliptical distribution. CDISC can be used to achieve a specified spanload distribution by setting the appropriate sectional lift coefficient at each design station, moving toward the elliptical minimum overall or removing local variations due to components such as engines. For many of the cases in the detailed design phase, however, the desired spanload is not elliptical, but has been modified based on structural considerations such as wing root bending moment (related to wing weight) and off-design aerodynamics, such as stall and cruise buffet. Also, for an aft-swept wing, shifting load inboard reduces the nose-down pitching moment of the aircraft and any associated trim drag. While the resulting target spanload is often provided from preliminary design studies, the new version of CDISC includes a constraint option that defines a smooth spanload distribution and also computes the wing root bending moment which could provide useful trade information in the preliminary design phase.

The next component of drag considered is wave drag resulting from the development of the supercritical rooftop over the forward upper surface of the wing and its sudden termination in a shock (see figure 10). The theoretical minimum is zero wave drag with the elimination of the shock, but in practice allowing a weak shock increases the lift while adding minimal drag, increasing the lift/drag ratio. There are three ways to reduce wave drag at a constant sectional lift that are built into the TPGEN flow constraint, shown in figure 10.

The first is to increase the adverse pressure gradient over the rooftop (more positive UDF), shifting the rooftop lift forward and reducing the shock strength at the aft end. The knowledge base built into this constraint limits the adverse gradient magnitude based on studies looking at when the rooftop would collapse and create a double shock, resulting in drag creep, especially at lower freestream Mach numbers and lift coefficients. One advantage of this approach is that it also decreases the magnitude of the nose down pitching moment, thus reducing trim drag.

A second approach is to shift the shock aft, adding length to the rooftop so that its level can drop to maintain the same lift. This method is limited by adverse effects on the boundary layer going through a steep gradient further aft, potentially leading to trailing edge separation. Moving the shock too far aft can also generate a local high-curvature region that can lead to more drag at higher Mach numbers and lift coefficients. One other factor relating to shock position is shock sweep. As the wave drag is related to the component of local Mach number normal to the shock (M_n), the shock location relative to adjacent design station values can lead to either more or less shock sweep, reducing or increasing the wave drag.

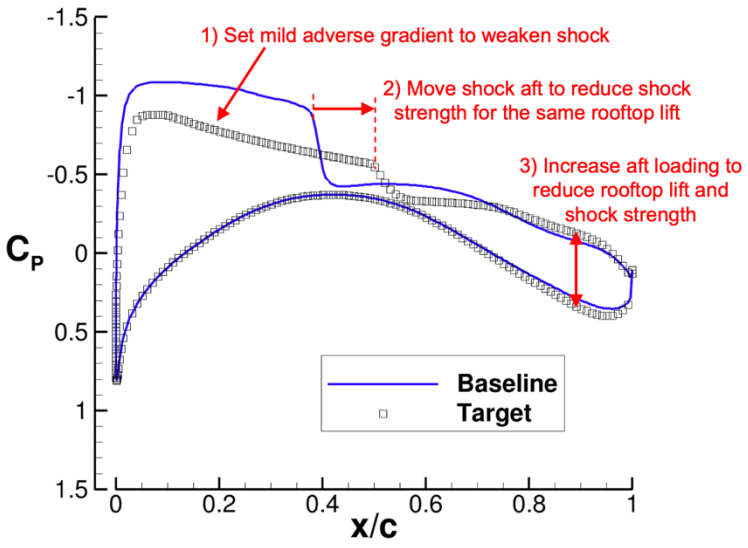

Figure 10 – TPGEN approaches to reducing wave drag.

A third approach using the TPGEN constraint is to increase the aft loading on the airfoil, so that extra lift is carried in a subsonic flow region, reducing the lift under the rooftop zone. This results in the typical large aft camber and associated nose-down pitching moment of a supercritical airfoil, which can lead to increased trim drag. The TPGEN constraint has rules that will limit the section pitching moment in light of these adverse effects.

Typically, all three of these approaches are used in CDISC to reduce wave drag. The new version of the design code has added smart constraint options in TPGEN that will adjust the values used by the three approaches during the design to try to lower M_n to a value of 1.05 or less to minimize wave drag.

The final component of drag addressed in CDISC is viscous drag related to the boundary layer state. For designs involving only turbulent flow, the primary concern is areas of flow separation. This is generally not an issue at the cruise point, though interference between the wing and other components such as the fuselage, engines, pylons, or struts (on a TTBW) can create local pockets of separation. However, the boundary layer thickness at the trailing edge does affect profile drag and can be an indicator of early drag rise and buffet at higher Mach numbers or lift coefficients. Some exploratory work is underway to include limits on skin friction coefficient at the trailing edge of the upper surface in the smart constraint options in TPGEN that limit shock Mach number and set pitching moment coefficient.

For designs utilizing NLF for viscous drag reduction, the TPGEN constraint automatically creates target pressures using the CATNLF method to obtain a specified extent of laminar flow (see figure 9, laminar case). The x1 point is moved forward based on the leading-edge sweep, chord Reynolds number, and the CF critical N-factor to create the rapid acceleration used to limit growth of the CF peak near the leading edge. The target pressure rooftop gradient, UDF, is then set based on the freestream Mach number, chord Reynolds number, desired transition location (for now, the same as the shock location x2), and the TS critical N-factor. At transonic speeds and moderate Reynolds numbers, this often yields a low value of UDF that also keeps the mid-chord CF growth suppressed, usually at the cost of a small increase in wave drag relative to a turbulent flow design. It should be noted that NLF designs reduce not only the skin friction drag but also the profile drag due to the thinner boundary layer over the aft part of the airfoil. At this time, the automated calculation of the UDF value to control TS growth is not available for supersonic NLF design as there are other modes of transition (oblique TS and traveling CF) that become dominant in the mid-chord region. The UDF value would need to be user-selected for supersonic NLF design cases.

While TPGEN is typically used for drag-reduction cases, other flow constraints are also available that alter target pressures directly by imposing limits or smoothing the targets in local areas. These are often used on body-type components such as the fuselage or in juncture areas where the flow is also determined by interference effects. Also, some geometry constraints have smart options that change input values (e.g., flap deflection angle) based on flow quantities like hinge-line pressure coefficient, sectional lift coefficient, extent of trailing edge separation, or main-element/flap load balance. These can also be used to impact drag at both cruise and off-design conditions or in the context of multiple design points, such as for fighter or supersonic transport configurations. Finally, the

aerodynamic designs are almost always done within the confines of geometry constraints such as thickness, leading-edge radius, twist smoothness, and surface curvature and smoothness. Currently there are over 20 flow and geometry constraints available for design in the new code.

B. Efficiency

Historically, CDISC has been 1-3 orders of magnitude faster than numerical optimization, depending on the optimization approach. The key factor contributing to the efficiency of CDISC is still the use of essentially the same prescribed sensitivity derivatives present in the original code. These derivatives were obtained from simple analytical expressions relating a change in pressure coefficient to a change in surface curvature for subsonic flow or a change in surface slope for supersonic flow, with a blend of the two near a local Mach number of 1. The fixed derivative approach not only eliminates the need for adjoint solver runs but allows geometry updates to be made from partially converged flow solutions. In addition, since the target pressure distributions are developed from the current analysis pressures at each design cycle, the flow solution and final target pressures can be converged simultaneously. This typically means that a design takes about 1-2x the time required for a converged analysis of the baseline configuration.

It was noted earlier that the KNOPTER and CODISC optimization approaches have been coupled with CDISC to take advantage of this efficiency as well as reduce the interactive engagement time for a user in selecting the best constraint input values. Hooker [69] estimated that, for one case, optimization provided a 3-5x reduction in the total design time relative to submitting multiple normal design runs after manually adjusting the input variables to improve aircraft performance. Our approach so far in the new version of CDISC is to add smart options to some flow and geometry constraints that will automatically adjust the constraint input values based on local flow variables and knowledge-based rules that generally relate the flow variable to an integrated quantity such as sectional drag (see discussion on smart constraints in the Effectiveness subsection above). However, these rules are not directly tied to a global aerodynamic quantity such as total drag and thus avoid the need to go to higher convergence levels in the flow solver runs to extract the sensitivity derivatives required for the optimization process. In addition, there has been an on-going philosophy in CDISC to build in rules based on multipoint considerations with the goal of reducing the need to redesign to improve off-design performance.

Finally, significant effort has gone into automatically setting underrelaxation factors for geometry and twist angle changes, as well as limits on flow and geometry parameters to increase the robustness of the design process. While this can perhaps extend some design run times, it makes obtaining a stable solution more likely overall and eliminates the need for manual adjustment and resubmission. Work also continues on the grid movement code, which is often the cause if the design process does fail, especially on complex geometries. Various improvements have been made to ensure a reasonable surface grid as well as more effective clean-up of negative volume grid cells, along with better diagnostic output to help identify problem areas.

C. Ease of Use

The final “E” of a good code, Ease of use, involves the time and effort required to set up a design case, run it, and interpret the results. Reflecting comments from Weston [100] about the old version of CDISC requiring a significant amount of time to come up the learning curve as a user, there is a focus on providing better documentation, including a new user manual, sample cases, and training materials for new users. In addition, the number and complexity of input files have been reduced and a set-up executor code (SUE) has been created that automatically creates these input files from a single, simple input file. The use of the SUE code will be further described in the next section, where it is used to set up a sample design case.

The ease-of-use aspect relative to running the design loop with the flow solver is obviously tied to the experience and complexity of the flow solver as well. Currently, there are sample run scripts set up for use with the NASA USM3D-ME and FUN3D flow solvers, which read in UGRID format [101] mixed-element grids and write out plotting files from which flow and geometry information is extracted. Prior experience indicates that developing converter modules for other flow solvers that utilize different formats is generally straight forward, if needed. The discussion at the end of the previous subsection on improving robustness also is very relevant to ease of use, hopefully providing more time to focus on analyzing design results.

Two graphics codes have been developed to help in the interpretation of both how the design case has been set up as well as how well the run did in terms of effectiveness in meeting the objectives for performance and convergence of the process. The first code, DISCPLOT, is used to display target and design pressures, along with the corresponding new geometries and geometric distributions such as curvature, camber, and thickness, for each component and design station for each design cycle. Spanwise plots of sectional characteristics such as lift and pitching moment, maximum thickness, leading-edge radius and twist are also available to allow the visualization of

the progression of the design through the design cycles. The second code, PREDISC, is used more for plotting the configuration as a whole, plotting original and design grids along with surface flow contours. This code is often used to confirm or assist in the setup of the design case, examine the design results between design stations or the effects on nearby components, or to visualize areas where the grid movement process had problems.

IV. Sample Design

A. Design Setup

To illustrate the use of the CDISC design method in a preliminary design context, a sample case will be set up and run to improve the performance of the CRM-M8 generic transonic transport. This configuration was developed by Hiller [91] by unsweeping the wing and scaling the overall dimensions of the CRM to more closely represent a single-aisle transport. A new baseline wing was then defined to reflect what might be created in a preliminary design process. A single airfoil, in this case one from mid-semispan on the CRM-M8 wing, was used to redefine the entire wing (except at the wing root) but with the thickness scaled to match the CRM-M8 spanwise thickness-to-chord ratio distribution, assuming that this distribution was derived from structural considerations. The wing was then given an initial twist based on a function of leading-edge sweep, with the final twist eventually being determined during the CDISC design process.

The SUE code was then used to set up the input files needed for the CDISC design. From a list of components consisting of one of more surface patch families in the sue.input file, a wing design component (green in figure 11) is defined with the default design station locations option placing 11 equally spaced stations from just outboard of the wing root to just inboard of the tip (black lines). The remaining components (mid-fuselage/fairing and wingtip, shown in red) listed in the sue.input file are designated as blend components that absorb the changes made at the ends of the design component.

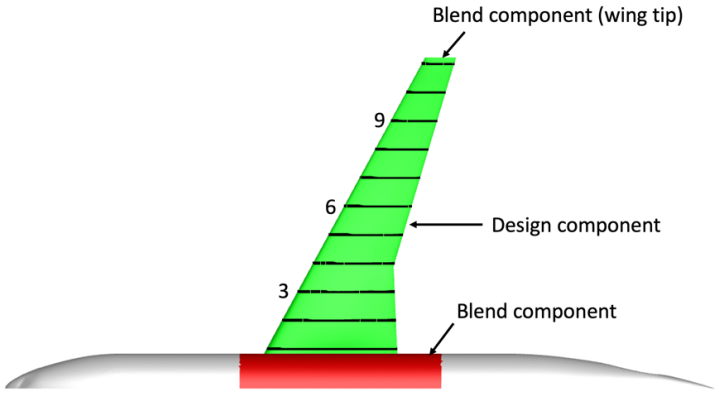

Figure 11 – CRM-M8 design case setup.

The sue.input file also contains flow information for the sample case, which are the same design conditions as used in Ref. 91 - a cruise Mach number of 0.8, Reynolds number per unit length of 0.1275 (21 million based on mean aerodynamic chord), and a lift coefficient of 0.543. This information is used by the SUE code to set up a default set of constraints based on best practices for a turbulent wing design. The key constraints and their effects on the design will be described next.

After setting the above flow parameters in CDISC with the SETFP constraint, the SETDP constraint is called to set several flow and geometry design parameters at each design station. The default input flow parameters set the sectional lift coefficient to the original baseline value and will use the smart constraint option to set the initial pitching moment coefficient based on the design lift coefficient, then increase the magnitude of that value, if needed, to keep the value of M_n less than 1.05. For the geometry constraints, the default thickness option will maintain the baseline value while the leading-edge radius option will set the radius-to-chord ratio to 0.7 times the maximum thickness-to-chord ratio squared. In addition to setting these parameters, the SETDP constraint automatically calls the THICK and LERAD constraints to enforce these values during the design, as well as calling an airfoil geometry smoothing constraint with a default number of smoothing cycles.

The next constraint written by SUE is the TPGEN flow constraint, with all of the input parameters set to default values. For many of our previous designs, a desired spanload was provided, often stated as maintaining the baseline spanload. The new constraint option that can specify a parabolic-type of spanload was considered for the design, but it was decided that a cleaner comparison with the baseline could be made by maintaining the original spanload here as well. A couple of variations of spanload using the new constraint option were also made to evaluate the new constraint, with a few comments on them in the Design Results subsection below.

The default values for two of the other TPGEN input parameters locate the beginning of the pressure rooftop (x1) based on a multiple of the leading-edge radius value set in LERAD and the end of the rooftop (x2, shock location) as a function of the freestream Mach number and the sweep of the shock. The shock location is determined by an iterative procedure with some modifications based on previous design experience that move the shock forward over the inboard part of the wing to increase the shock sweep. The default UDF values that determine the rooftop slope at each station are initially set based on results from the CODISC studies in Ref. 74, with higher values inboard and lower outboard. These values, along with the pitching moment as described above, are adjusted as needed to keep the value of M_n below 1.05. As mentioned in the Method section, the resulting target pressure distributions are then adjusted to match the desired lift and pitching moment coefficients at each station.

In addition to the thickness and leading-edge radius constraints called by SETDP, two more geometry constraints are written by the SUE code as part of the standard set for a transonic turbulent wing design. The CCURV constraint is used to limit the minimum and maximum levels of streamwise curvature in the region between x/c = 0.3 and 0.8 where the shock is located as this was found to improve performance at near-cruise off-design conditions. The other constraint smoothes the wing twist distribution, which generally helps the aerodynamics as well as simplifies the manufacture of the wing.

One other constraint was used that substitutes an entirely new airfoil for the current one at a station. For this case setup, the final design station is too close to the tip for CDISC design to be effective because the pressures there are strongly influenced by the tip vortex roll-up. In order to maintain a smooth geometry in the tip region, the airfoil at the final station is replaced with the current airfoil from the adjacent station. The twist of the new airfoil is extrapolated from the previous 2 stations to keep the twist distribution smooth. All of the above flow and geometry input is created from a simple sue.input file that is less than 10 lines long, reflecting the setup aspect of ease of use for the design method.

B. Design Results

The design case was initiated by obtaining a flow solution for the baseline grid converged to a lift coefficient of 0.543 using the internal lift-matching capability in USM3D-ME. The CDISC design process was then restarted from this solution and run for 60 design cycles, with 30 flow iterations per design cycle for a total of 1800 flow iterations beyond the 3000 used for the baseline analysis. The design was very stable at this point, matched the target pressures fairly well, and was representative of the typical efficiency of CDISC with the design taking about the same time as the baseline analysis.

Figure 12 shows the final design pressures compared with both the baseline values and the target pressure distributions, along with the corresponding airfoils with the twist removed, at design stations 3, 6, and 9 (see figure 11). The baseline and design airfoils have very similar shapes and produce the aft loading in the pressures that is characteristic of supercritical airfoils. The primary difference in the pressures is in the rooftop region, where the baseline flow, after an initial shock, reaccelerates to a moderate shock that is located further aft than in the design case. The target rooftop pressure gradient can be seen to flatten for the outboard stations, reflecting the best practice found in the CODISC study. The design rooftop flow at all three stations terminates in a weak shock, with M_n values around 1.05, creating very little wave drag. Close examination of the pressure coefficients at the trailing edge shows that the design pressure coefficients are slightly more positive than the baseline values, suggesting that the boundary layer is thinner there for the design, which could indicate a slight improvement in profile drag as well.

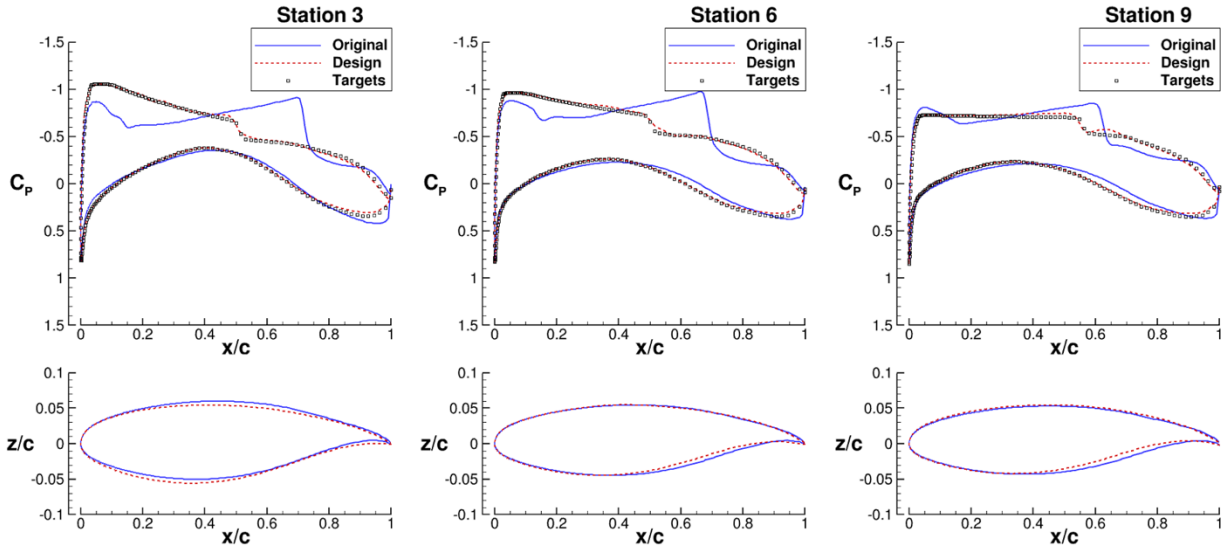

a) Station 3 b) Station 6 c) Station 9

Figure 12 – Pressures distributions and airfoils at 3 design stations.

The spanwise lift and pitching moment distributions are shown in figure 13. The design wing (red) has essentially the same lift distribution as the baseline (blue), suggesting no induced drag change for the design relative to the baseline. The spanwise variation of sectional pitching moment coefficients shown in figure 13b indicates that the design has a much more typical distribution than the baseline, with lower values inboard and higher values outboard to help protect against stall and buffet. Note that much of the increase in nose-down pitching moment at the inboard stations for the baseline is largely due to the lift created by the moderate shock located behind mid-chord and not so much due to a loading difference from the aft camber. These higher sectional pitching moments would lead to more trim drag for the baseline configuration in a full aircraft design.

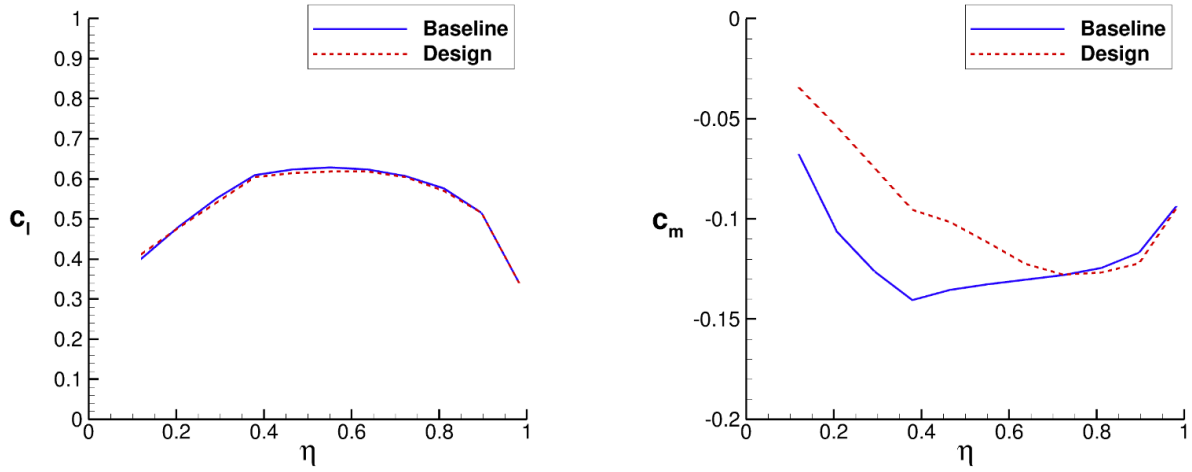

a) Sectional lift coefficient. b) Sectional pitching moment coefficient

Figure 13 – Spanwise flow characteristics.

The spanwise geometry characteristics are plotted in figure 14 and show that the sectional thickness values were maintained during the design as requested, and also that the specifying of the leading-edge radius as a function of thickness gave values similar to the baseline. The initial twist distribution that was based on the leading edge sweep of the wing matched the final distribution fairly well except at the root, providing a good starting point for the design. The final twist distribution was driven by the difference between the target and design pressures on the upper surface near the leading edge at each design station, with some twist smoothing also applied.

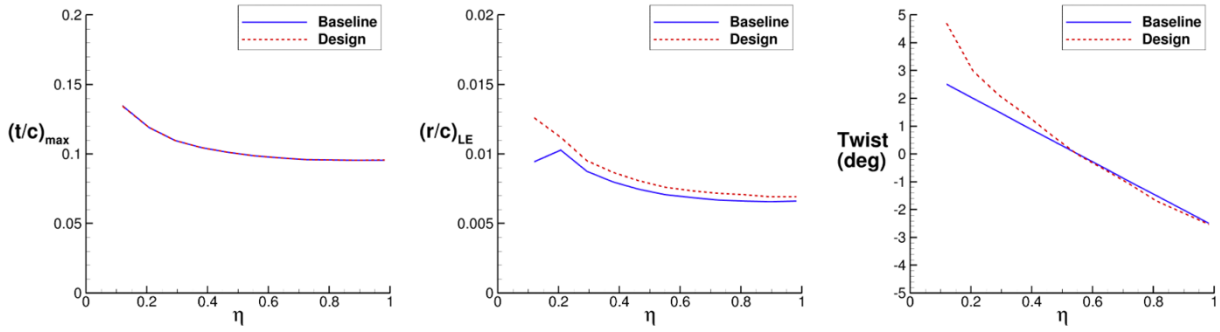

a) Maximum thickness/chord b) Leading edge radius/chord c) Twist, degrees

Figure 14 – Spanwise geometry characteristics.

Overall, the design reduced the drag by over 19 counts, or about 7.5% relative to the baseline wing/body drag. As suggested above, this was due largely to reduced shock strengths leading to less wave drag, with perhaps some profile drag improvement. For this case, the induced drag was held fixed by specifying the same target spanload as the baseline. To investigate potential induced drag effects, a couple of test designs were also run to check the new parabolic-type spanload constraint. Cases were run for spanload function exponents of 2 and 4, with 4 approximating an elliptical distribution and 2 carrying more load inboard, with the baseline spanload similar to an exponent of 3 spanload. The exponent 4 case had a drag reduction of about 1.5 counts relative to the design that maintained the baseline spanload, but an increase of 28% in root bending moment. The exponent 2 case had a larger drag increase, 6.7 counts, but reduced the root bending moment by 26%, relative to the original design. Although these are just preliminary results, they indicate that the new constraint option could provide useful information for making performance versus weight trades.

The primary point of this example, however, was not just demonstrating a drag reduction approach, but that a reasonable preliminary design baseline can be significantly improved with a process that is easy to use with rapid turnaround. CDISC can be used in the preliminary design context to accurately evaluate the effects of varying common flow and geometry parameters or in the application of new technologies such as NLF, cruise slotted airfoils, or truss-braced wings where the details of the flow in local areas are very important to the performance.

V. Concluding Remarks

Frankly, it has been surprising that the CDISC design method has lasted this long in view of the other good design methods that have been developed. Certainly tying it to the latest flow solver and grid technologies, many of which were freely available to US entities, made it an attractive option for design with these codes. When the knowledge base was available for a particular design problem, the efficiency of the code relative to numerical optimization was also a draw for its use. For designs outside of the knowledge base, the challenge of understanding the flow physics, developing new rules to drive the design process, and seeing it successfully applied to improve the vehicle was actually one of the more enjoyable parts of the process. This more often than not occurred as a cooperative effort with researchers in industry or at other government centers and was successful largely due to the experienced aerodynamicists that gave ideas for improvements and feedback on the results.

While a number of times CDISC gave performance improvements similar to optimization, the view of the authors has always been that the two approaches were complementary. Especially in areas where the knowledge base wasn't established, optimization results were a good source of ideas for both flow and geometry constraints. Interestingly,

users often suggested this dual use, but sometimes came from opposite directions. One would suggest getting the design close using the speed of CDISC, then refining the design with optimization to squeeze out the final improvement. Another thought was that optimization could do most of the work, then CDISC could be used to clean up any undesirable features in the final pressure distributions and/or geometry. Both have worked in the past and seem like a good approach for the future.

Looking ahead to the future, the CDISC development effort continues to focus on the efficiency, effectiveness, and ease of use of the method. The new design system software is currently in the approval process for dissemination. While the design example included in this paper illustrated the use of CDISC in a preliminary design environment, the primary use of CDISC from the perspective of the CDISC team at NASA LaRC has been its application in the detailed design of new concepts and the use of new technologies. The four companion papers to this one in Refs. 89,91,93,95 to this one give good examples of these types of applications. The challenges of new economic and environmental realities should provide many more opportunities for aerodynamic design, and hopefully CDISC can continue to evolve to meet those challenges.

Acknowledgments

This work was sponsored by the NASA Advanced Air Transport Technology (AATT) Project, which is part of the Advanced Air Vehicles Program (AAVP) in the NASA Aeronautics Research Mission Directorate (ARMD). Resources supporting some computational results in this paper were provided by the NASA High-End Computing (HEC) Program through the NASA Advanced Supercomputing (NAS) Division. A special thanks to all of the CDISC users over the years that have been enjoyable to work with in developing and applying the design method.

References

[1] Jameson, Antony, "CFD for Aerodynamic Design and Optimization," AIAA 2003-3438, June 2003.
[2] Tinoco, E.N., "The Changing Role of Computational Fluid Dynamics in Aircraft Development," AIAA-98-2512, June 1998. https://doi.org/10.2514/6.1998-2512
[3] Johnson, F.T., and Tinoco, E.N., "Thirty Years of Development and Application of CFD at Boeing Commercial Airplanes, Seattle," AIAA 2003-3439, June 2003. https://doi.org/10.2514/6.2003-3439
[4] Bauer, F.; Garabedian, P.; Korn, D.; and Jameson, A.: Supercritical Wing Sections 11. Lecture Notes in Economics and Mathematical Systems, Vol. 108, Springer-Verlag, New York, 1975.
[5] Jameson, A., Caughey, D.A., Newman, P.A., and Davis, R.M., "A Brief Description of the Jameson-Caughey NYU Transonic Swept-Wing Computer Program – FLO22". NASA TMX-73996, 1976.
[6] Boppe, C. W., "Aerodynamic Analysis for Aircraft With Nacelles, Pylons and Winglets at Transonic Speeds", NASA CR-4066, 1987.
[7] Mann, M.J., Campbell, R.L., and Ferris, J.C., "Aerodynamic Design for Improved Maneuverability by the Use of Three-Dimensional Transonic Theory," AIAA 1983-1859, July 1983. https://doi.org/10.2514/6.1983-1859
[8] Mann, M.J., "The Design of Supercritical Wings by the Use of Three-Dimensional Transonic Theory," NASA TP-1400, February 1979.
[9] Barger, R.L., and Brooks, C.W., Jr., "A Streamline Curvature Method for Design of Supercritical and Subcritical Airfoils," NASA TN D-7770, September 1974.
[10] Davis, W.H., Jr., "Technique for Developing Design Tools from the Analysis Methods of Computational Aerodynamics," AIAA 1979-1529, July 1979. https://doi.org/10.2514/6.1979-1529
[11] Jameson, A., and Caughey, D.A., "A Finite Volume Method for Transonic Potential Flow Calculations", A Collection of Technical Papers – AIAA 3rd Computational Fluid Dynamics Conference, pp. 35-54, June 1977.
[12] Campbell, R.L., and Smith, L.A., "A Hybrid Algorithm for Transonic Airfoil and Wing Design," AIAA 87-2552, August 1987. https://doi.org/10.2514/6.1987-2552
[13] Campbell, R.L., Waggoner, E.G., and Phillips, P.S., "Design of a Natural Laminar Flow Wing for a Transonic Corporate Transport," AIAA 1986-314, January 1986. https://doi.org/10.2514/6.1986-314
[14] Melson, N.D., and Streett, C.L., "TAWFIVE: A User's Guide", NASA TM-84619, September 1983.
[15] Waggoner, E.G., Campbell, R.L., and Phillips, P.S., "Computational Wing Design in Support of an NLF Variable Sweep Transition Flight Experiment," AIAA-85-4074, October 1985. https://doi.org/10.2514/6.1985-4074
[16] Anderson, Bianca Trujilo, and Meyer, Robert R., Jr., "Effects of Wing Sweep on In-Flight Boundary-Layer Transition for a Laminar Flow Wing at Mach Numbers From 0.60 to 0.79", NASA TM-101701, July 1990.
[17] Chen, H. C., Yu, N. J., Rubbert, P. E., and Jameson, A., "Flow Simulations for General Nacelle Configurations Using Euler Equations," AlAA Paper 83-0539. 1983.
[18] Lin, W.F., Chen, A.W., and Tinoco, E.N., "3D Transonic Nacelle and Winglet Design," AIAA-90-3064-CP, September 1990. https://doi.org/10.2514/6.1990-3064
[19] Bell, R.A., and Cedar, R.D., "An Inverse Method for the Aerodynamic Design of Three-Dimensional Aircraft Engine Nacelles," A92-13958, October 1991.

[20] Thomas, J. L., Van Leer, B., and Walters R. W., "Implicit Flux-Split Schemes for the Euler Equations", AIAA 85-1680, July 1985.
[21] Chen, H.C., "An Installed Nacelle Design Method Using Multiblock Euler Solver," AIAA-93-0528, January 1993. https://doi.org/10.2514/6.1993-528
[22] Wie, Y.-S., Collier, F.S., Jr., Wagner, R.D., Viken, J.K., and Pfenninger, W., "Design of a Hybrid Laminar Flow Control Nacelle," AIAA 1992-400, January 1992. https://doi.org/10.2514/6.1992-400
[23] Vatsa, V.N., and Wedan, B.W., "Development of an Efficient Multigrid Code for 3-D Navier-Stokes Equations," AIAA Paper 89-1791, 1989.
[24] Yu, N.J., and Campbell, R.L., "Transonic Airfoil and Wing Design Using Navier-Stokes Codes," AIAA-92-2651-CP, June 1992. https://doi.org/10.2514/6.1992-2651
[25] Shmilovich, A., Lynch, F.T., and Pelkman, R.A., "A CFD-Based Design Strategy for Advanced Transonic Wing Concepts with Practical Ramifications for Subsonic Transports," AIAA 1993-2946, July 1993. https://doi.org/10.2514/6.1993-2946
[26] Jou, W.H., Huffman, W.P., and Young, D.P., "Practical Considerations in Aerodynamic Design Optimization," AIAA-95-1730-CR, June 1995. https://doi.org/10.2514/6.1995-1730
[27] Walatka, Pamela P., Buning, Pieter G., Pierce, Larry, and Elson, Patricia A., "PLOT3D User's Manual", NASA TM 101067, March 1990.
[28] Thomas, J.L., Taylor, S.L., and Anderson, W.K.: , "Navier-Stokes Computations of Vortical Flows Over Low Aspect Ratio Wings", AIAA-87-0207, 1987.
[29] Buning, P. G., Parks, S. J., Chan, W. M., and Renze, K. J., "Application of the Chimera Overlapped Grid Scheme to Simulation of Space Shuttle Ascent Flows", Presented at the 4th International Symposium on Computational Fluid Dynamics, Davis, CA, September 9-12,1991.
[30] Naik, D.A., Krist, S.E., Campbell, R.L., Vatsa, V.N., Buning, P.G., and Gea, L.M., "Inverse Design of Nacelles Using Multi-Block Navier Stokes Codes," AIAA-95-1820-CR, June 1995. https://doi.org/10.2514/6.1995-1820
[31] Campbell, R.L., "An Approach to Constrained Aerodynamic Design with Application to Airfoils," NASA-TP-3260, November 1992.
[32] Campbell, R.L., "Efficient Constrained Design Using Navier-Stokes Codes," AIAA-95-1808-CP, June 1995. https://doi.org/10.2514/6.1995-1808
[33] Campbell, R.L., "Efficient Viscous Design of Realistic Aircraft Configurations," AIAA-98-2539, June 1998. https://doi.org/10.2514/6.1998-2539
[34] Liebeck, R.H., Page, M.A., and Rawdon, B.K., "Blended-Wing-Body Subsonic Commercial Transport," AIAA-98-0438, January 1998. https://doi.org/10.2514/6.1998-438
[35] Potsdam, M.A., Page, M.A., and Liebeck, R.H., "Blended Wing Body Analysis and Design," AIAA-97-2317, June 1997. https://doi.org/10.2514/6.1997-2317
[36] Campbell, R.L., and Mann, M.J., "TLNS3D/CDISC Multipoint Design of the TCA Concept", NASA CP-1999-209691, Volume 1, Part 1, pp. 561-587, December 1999.
[37] Krist, S.E., Bauer, S.X.S., Campbell, R.L., "Viscous Design of TCA Configuration", NASA CP-1999-209692 Volume 1, Part 1, pp. 1043-1069, December 1999.
[38] Anders, S.G, and Fischer, M.C., "F-16XL-2 Supersonic Laminar Flow Control Flight Test Experiment", NASA TP-1999-209683, December 1999.
[39] Frink, N.T., "Assessment of an Unstructured-Grid Method for Predicting 3-D Turbulent Viscous Flows", AIAA-96-0292, January 1996.
[40] Anderson, W.K., and Bonhaus, D.L., "An Implicit Upwind Algorithm for Computing Turbulent Flows on Unstructured Grids", Computers and Fluids, Vol. 23, No.1,1994, pp. 1-21.
[41] Parikh, P., "Development of a Modular Aerodynamic Design System Based on unstructured Grids," AIAA-97-0172, January 1997. https://doi.org/10.2514/6.1997-172
[42] Olsen, M.E., Driver, D.M., Schairer, E.T., Naughton, J., "The ROCK (AST-1) Wing: Design, Experiment and Computation," AIAA 2000-0670, January 2000. https://doi.org/10.2514/6.2000-670
[43] Roman, D., Allen, J.B., and Liebeck, R.H., "Aerodynamic Design Challenges of the Blended-Wing-Body Subsonic Transport," AIAA-2000-4335, August 2000. https://doi.org/10.2514/6.2000-4335
[44] Roman, D., Gilmore, R., and Wakayama, S., "Aerodynamics of High-Subsonic Blended-Wing-Body Configurations," AIAA 2003-554, January 2003. https://doi.org/10.2514/6.2003-554
[45] Campbell, R.L., Carter, M.B., Pendergraft, O.C., Jr., Friedman, D.M., and Serrano, L., "Design and Testing of a Blended Wing Body with Boundary Layer Ingestion Nacelles at High Reynolds Numbers (Invited)," AIAA 2005-459, January 2005. https://doi.org/10.2514/6.2005-459
[46] Wahls, R., "High Speed Slotted Wing Technology," NASA Vehicle Systems Program Annual Meeting, 2004.
[47] Whitcomb, R. T., and Clark, L. R., "An Airfoil Shape for Efficient Flight at Supercritical Mach Numbers," NASA/TM-X-1109, July 1965.
[48] Johnson, F. T., Samant, S.S., Bieterman, M.B., Melvin, R.G., Young, D.P., Bussoletti, J.E., and Hilmes, C.L., "TranAir: a Full-Potential, Solution-Adaptive, Rectangular Grid Code for Predicting Subsonic, Transonic, and Supersonic Flows About Arbitrary Configurations - Theory Document", NASA Contractor Report CR-4348, December 1992.
[49] McLean, J. D., Witkowski, D. P., and Campbell, R. L., "Slotted Aircraft Wing," U.S. Patent No. 7,048,235, May 2006.

[50] Vassberg, J. C., Gea, L.-M., McLean, J. D., Witowski, D. P., Krist, S. E., and Campbell, R. L., "Slotted Aircraft Wing," U.S. Patent No. 7,048,228, May 2006.
[51] Re, R.J., Pendergraft, O.C., Jr., and Campbell, R.L., "Low Reynolds Number Aerodynamic Characteristics of Several Airplane Configurations Designed to Fly in the Mars Atmosphere at Subsonic Speeds," NASA/TM-2006-214312, August 2006.
[52] Washburn, A.E., Gorton, S.A, and Anders, S.G., "A Snapshot of Active Flow Control Research at NASA Langley," AIAA Paper 2002-3155, June 2002. https://doi.org/10.2514/6.2002-3155.
[53] Milholen, W.E., II, and Owens, L.R., "On the Application of Contour Bumps for Transonic Drag Reduction (Invited)," AIAA Paper 2005-0462, January 2005. https://doi.org/10.2514/6.2005-462.
[54] Gally, T., and Campbell, R. L., "Constrained Aerothermodynamic Design of Hypersonic Vehicles," AIAA Paper 2002-3139, June 2002. https://doi.org/10.2514/6.2002-3139.
[55] Bezos-O'Connor, G.M., Mangelsdorf, M.F., Maliska, H.A., Washburn, A.E., and Wahls, R.A., "Fuel Efficiencies through Airframe Improvements," AIAA Paper 2011-3530, June 2011. https://doi.org/10.2514/6.2011-3530.
[56] Campbell, R. L., Campbell, M. L, and Streit, T., "Progress Toward Efficient Laminar Flow Analysis and Design," AIAA Paper 2011-3527, June 2011. https://doi.org/10.2514/6.2011-3527.
[57] Aftosmis, M.J., Berger, M.J., and Adomavicius, G., "A Parallel Multilevel Method for Adaptively Refined Cartesian Grids with Embedded Boundaries," AIAA Paper 2000-808, August 2000. https://doi.org/10.2514/6.2000-808.
[58] Ishikawa, H., Ueda, Y., and Tokugawa, N., "Natural Laminar Flow Wing Design for a Low-Boom Supersonic Aircraft," AIAA Paper 2017-1860, January 2017. https://doi.org/10.2514/6.2017-1860.
[59] Campbell, R. L., and Lynde, M. N., "Expanding the Natural Laminar Flow Boundary for Supersonic Transports," AIAA Paper 2016-4327, June 2016. https://doi.org/10.2514/6.2016-4327.
[60] Vassberg, J., Dehaan, M., Rivers, M., and Wahls, R., "Development of a Common Research Model for Applied CFD Validation Studies," AIAA Paper 2008-6919, August 2008. https://doi.org/10.2514/6.2008-6919.
[61] Campbell, R. L., and Lynde, M. N., "Natural Laminar Flow Design for Wings with Moderate Sweep," AIAA Paper 2016-4326, June 2016. https://doi.org/10.2514/6.2016-4326.
[62] Crouch, J.D., Sutanto, M.I., Witkowski, D.P., Watkins, A.N., Rivers, M.B., and Campbell, R. L., "Assessment of the National Transonic Facility for Natural Laminar Flow Testing," AIAA Paper 2010-1302, January 2010. https://doi.org/10.2514/6.2010-1302.
[63] Campbell, R. L., and Lynde, M. N., "Building a Practical Natural Laminar Flow Design Capability," AIAA Paper 2017-3059, June 2017. https://doi.org/10.2514/6.2017-3059.
[64] Lynde, M. N., and Campbell, R. L., "Computational Design and Analysis of a Transonic Natural Laminar Flow Wing for a Wind Tunnel Model," AIAA Paper 2017-3058, June 2017. https://doi.org/10.2514/6.2017-3058.
[65] Lynde, M. N., Campbell, R. L., Rivers, M.B., Viken, S. A., Chan, D.T., Watkins, A.N., and Goodliff, S.L., "Preliminary Results from an Experimental Assessment of a Natural Laminar Flow Design Method," AIAA Paper 2019-2298, January 2019. https://doi.org/10.2514/6.2019-2298.
[66] Lynde, M. N., Campbell, R. L., and Viken, S. A., "Additional Findings from the Common Research Model Natural Laminar Flow Wind Tunnel Test," AIAA Paper 2019-3292, June 2019. https://doi.org/10.2514/6.2019-3292.
[67] Zuene, C.H., "Enabling Speed Agility for the Air Force," AIAA Paper 2012-349, June 2012. https://doi.org/10.2514/6.2012-349.
[68] Wick, A.T., Hooker, J.R., Zuene, C.H., Jones, G., and Milholen, W.E., II, "Design and Transonic Wind Tunnel Testing of a Cruise Efficient STOL Military Transport," AIAA Paper 2013-1100, January 2013. https://doi.org/10.2514/6.2013-1100.
[69] Wick, A.T., Hooker, J.R., Zuene, C.H., and Agelastos, A., "Over Wing Nacelle Installations for Improved Energy Efficiency," AIAA Paper 2013-2920, June 2013. https://doi.org/10.2514/6.2013-2920.
[70] Wick, A.T., Hooker, J.R., and Zuene, C.H., "Integrated Aerodynamic Benefits of Distributed Propulsion," AIAA Paper 2015-1500, January 2015. https://doi.org/10.2514/6.2015-1500.
[71] Hooker, J.R., "Design of a Hybrid Wing Body for Fuel Efficient Air Mobility Operations at Transonic Flight Conditions," AIAA Paper 2014-1285, January 2014. https://doi.org/10.2514/6.2014-1285.
[72] Wick, A.T., Hooker, J.R., Walker, J., Chan, D.T., Plumley, R.W., and Zuene, C.H., "Hybrid Wing Body Performance Validation at the National Transonic Facility," AIAA Paper 2017-0099, January 2017. https://doi.org/10.2514/6.2017-0099.
[73] Chan, D.T., Hooker, J.R., Wick, A.T., Plumley, R.W., Zuene, C.H., Ol, M.V., and DeMoss, J. A., "Transonic Semispan Aerodynamic Testing of the Hybrid Wing Body with Over Wing Nacelles in the National Transonic Facility," AIAA Paper 2017-0098, January 2017. https://doi.org/10.2514/6.2017-0098.
[74] Campbell, R.L., and Lynde, M. N., "A Knowledge-Based Optimization Method for Aerodynamic Design," AIAA Paper 2019-1207, January 2019. https://doi.org/10.2514/6.2019-1207.
[75] Smith, S.C., Nemec, M. and Krist, S.E., "Integrated Nacelle-Wing Shape Optimization for an Ultra-High Bypass Fanjet Installation on a Single-Aisle Transport Configuration," AIAA Paper 2013-0543, January 2013. https://doi.org/10.2514/6.2013-0543.
[76] Milholen, W.E., II, Jones, G.S., and Cagle, C.M., "NASA High-Reynolds Number Circulation Control Research - Overview of CFD and Planned Experiments (Invited)," AIAA Paper 2010-344, January 2010. https://doi.org/10.2514/6.2010-344.
[77] Milholen, W.E., II, Jones, G.S., Chan, D.T., and Goodliff, S.L., "High-Reynolds Number Circulation Control Testing in the National Transonic Facility (Invited)," AIAA Paper 2012-0103, January 2012. https://doi.org/10.2514/6.2012-103.

[78] Jones, G.S., Milholen, W.E., II, Chan, D.T., Allan, B.G., Goodliff, S.L., Melton, L., Anders, S.G., Carter, M.B., and Capone, F., "Development of the Circulation Control Flow Scheme used in the NTF Semi-Span FAST-MAC Model," AIAA Paper 2013-3048, June 2013. https://doi.org/10.2514/6.2013-3048.
[79] Jones, G.S., Milholen, W.E., II, Chan, D.T., Melton, L., Goodliff, S.L., and Cagle, C.M., "A Sweeping Jet Application on a High Reynolds Number Semispan Supercritical Wing Configuration," AIAA Paper 2017-3044, June 2017. https://doi.org/10.2514/6.2017-3044.
[80] Jones, G.S., Milholen, W.E., II, Chan, D.T., Goodliff, S.L., Cagle, C.M., and Fell, J.S., "A Discrete and Distributed Steady Blowing Application on a High Reynolds Number Semispan Supercritical Wing Configuration (Invited)," AIAA Paper 2018-1138, January 2018. https://doi.org/10.2514/6.2018-1138.
[81] Rumsey, C.L., Neuhart, D.H., and Kegerise, M.A., "The NASA Juncture Flow Experiment: Goals, Progress, and Preliminary Testing (Invited)," AIAA Paper 2016-1557, January 2016. https://doi.org/10.2514/6.2016-1557.
[82] Viken, J.K., Viken, S.A., Deere, K. A., and Carter, M.B., "Design of the Cruise and Flap Airfoil for the X-57 Maxwell Distributed Electric Propulsion Aircraft," AIAA Paper 2017-3922, June 2017. https://doi.org/10.2514/6.2017-3922.
[83] Fredericks, W.J., McSwain, R.G., Beaton, B.F., Klassman, D.W., and Theodore, C.R., "Greased Lightning (GL-10) Flight Test Campaign," NASA/TM-2017-219643, July 2017.
[84] Campbell, R.L., Viken, S.A., and Lynde, M. N., "Application of Passive Drag Reduction Methods to a Generic Strut-Braced Wing," Platform For Aircraft Drag Reduction Innovation Workshop, December 2017.
[85] Kenway, G.K.W., Housman, J.A., and Kiris, C., "NASA Ames Research Center Contributions to the PADRI Workshop," Platform For Aircraft Drag Reduction Innovation Workshop, December 2017.
[86] Campbell, R.L., and Nayani, S. N., "Unstructured Grids for Sonic Boom Analysis and Design," AIAA Paper 2015-1250, January 2015. https://doi.org/10.2514/6.2015-1250.
[87] Pandya, M.J., Diskin, B., Thomas, J.L., and Frink, N.T., "Assessment of USM3D Hierarchical Adaptive Nonlinear Iteration Method Preconditioners for Three-Dimensional Cases," *AIAA Journal*, Vol. 55, No. 10, 2017, pp. 3409–3424. https://doi.org/10.2514/1.J055823.
[88] Lynde, M. N., Campbell, R. L., Hiller, B. R., and Owens, L. R., "Design of a Crossflow Attenuated Natural Laminar Flow Flight Test Article," AIAA Paper 2021-0173, January 2021. https://doi.org/10.2514/6.2021-0173.
[89] Banchy, M. N., Campbell, R. L., Hiller, B. R., and Bozeman, M.D., "CDISC Remote Design Method to Simulate Aircraft Interference Effects for the CATNLF Flight Test," AIAA Paper 2024-XXXX, January 2024. https://doi.org/10.2514/6.2024-XXXX.
[90] Hiller, B. R., Campbell, R., Lynde, M. N., and Boyett, T. K., "Design Exploration of a Transonic Cruise Slotted Airfoil," AIAA Paper 2021-2525, June 2021. https://doi.org/10.2514/6.2021-2525.
[91] Hiller, B. R., Campbell, R. L., and Banchy, M. N., "Transonic Cruise Slotted Wing Design for Commercial Transport Aircraft using CDISC," AIAA Paper 2024-XXXX, January 2024. https://doi.org/10.2514/6.2024-XXXX.
[92] Lynde, M. N., Campbell, R. L., and Hiller, B. R., "A Design Exploration of Natural Laminar Flow Applications for the SUSAN Electrofan Concept," AIAA Paper 2022-2303, January 2022. https://doi.org/10.2514/6.2022-2303.
[93] Pomeroy, B.W., Campbell, R. L., Banchy, M. N., and Hiller, B. R., "Application of the CATNLF Design Method to a Transonic Transport Empennage using CDISC," AIAA Paper 2024-XXXX, January 2024. https://doi.org/10.2514/6.2024-XXXX.
[94] Lockheed Martin, "X-59 Shaping the Future of Aviation," retrieved Nov. 2023. URL: https://www.lockheedmartin.com/en-us/products/x-59-quiet-supersonic.html
[95] Bozeman, M.B., Campbell, R. L., and Banchy, M. N., "Progress Towards the Design of a Natural Laminar Flow Wing for a Low-Boom Concept using CDISC," AIAA Paper 2024-XXXX, January 2024. https://doi.org/10.2514/6.2024-XXXX.
[96] Castner, R., Simerly, S., and Rankin, M., "Supersonic Inlet Test for a Quiet Supersonic Transport Technology Demonstrator in the NASA Glenn 8-foot by 6-foot Supersonic Wind Tunnel," AIAA Paper 2018-2850, June 2018. https://doi.org/10.2514/6.2018-2850.
[97] NASA, "Next Generation Experimental Aircraft Becomes NASA's Newest X-Plane," retrieved Nov. 2023. URL: https://www.nasa.gov/news-release/next-generation-experimental-aircraft-becomes-nasas-newest-x-plane/
[98] Droney, C. K., Sclafani, A. J., Harrison, N. A., Grasch, A. D., and Beyar, M. D., "Subsonic Ultra Green Aircraft Research: Phase III - Mach 0.75 Transonic Truss-Braced Wing Design," NASA/CR-2020-5005698, September 2020.
[99] Breaking Defense, "Air Force Picks Startup JetZero to Build Blended Wing Body Demonstrator," retrieved Nov. 2023. URL: https://breakingdefense.com/2023/08/air-force-picks-startup-jetzero-to-build-blended-wing-body-demonstrator/
[100] Weston, D.B., and Zuene, C.H., "Exercise of Knowledge-Based Aerodynamic Design Process on the AFRL SUGAR Model," AIAA Paper 2022-3661, June 2022. https://doi.org/10.2514/6.2022-3661.
[101] Mississippi State Center for Advanced Vehicular Systems, "UG_IO Software," retrieved Nov. 2023. URL: https://www.simcenter.msstate.edu/software/documentation/ug_io/3d_grid_file_type_ugrid.html